Much Excitement About Nothing?

adapted freely from William Shakespeare

Elastic and transition form factors

↙ ↘

Probe the excited nucleon structures at perturbative and nonperturbative QCD scales

Distinctive information on the roles played by DCSB and confinement in QCD

Quark-Gap Equation in QCD

The propagator can be obtained from QCD's gap equation: the Dyson-Schwinger equation (DSE) for the dressed-fermion self-energy, which involves the set of infinitely many coupled equations.

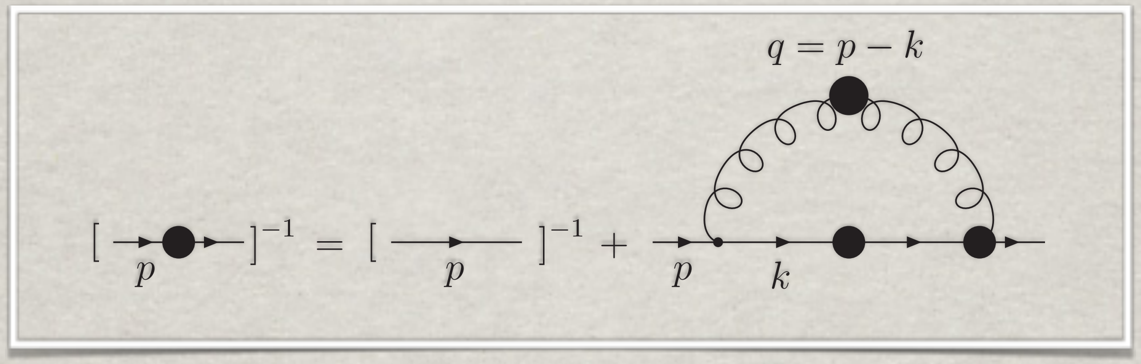

$$
\begin{aligned}
S^{-1}(p) &= Z_2(i\gamma\cdot p + m^{\rm bm}) + \Sigma(p) \;:=\; i\gamma\cdot p\, A(p^2) + B(p^2) \\
\Sigma(p) &= Z_1 \int^{\Lambda} \frac{d^4q}{(2\pi)^4}\, g^2 D_{\mu\nu}(p-q) \frac{\lambda^a}{2}\gamma_\mu S(q)\Gamma^a_\nu(q,p)
\end{aligned}
$$

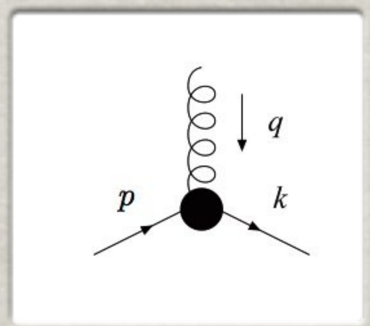

with the *running* mass function $M(p^2) = B(p^2)/A(p^2)$.

$D_{\mu\nu}$	:	dressed-gluon propagator
$\Gamma^a_\nu(q,p)$	:	dressed quark-gluon vertex
Z_2	:	quark wave function renormalization constant
Z_1	:	quark-gluon vertex renormalization constant

Each satisfies it's own DSE !

$$S^{-1}(p)|_{p^2=\zeta^2} = i\gamma\cdot p + m(\zeta)$$

where ζ is the renormalization point.

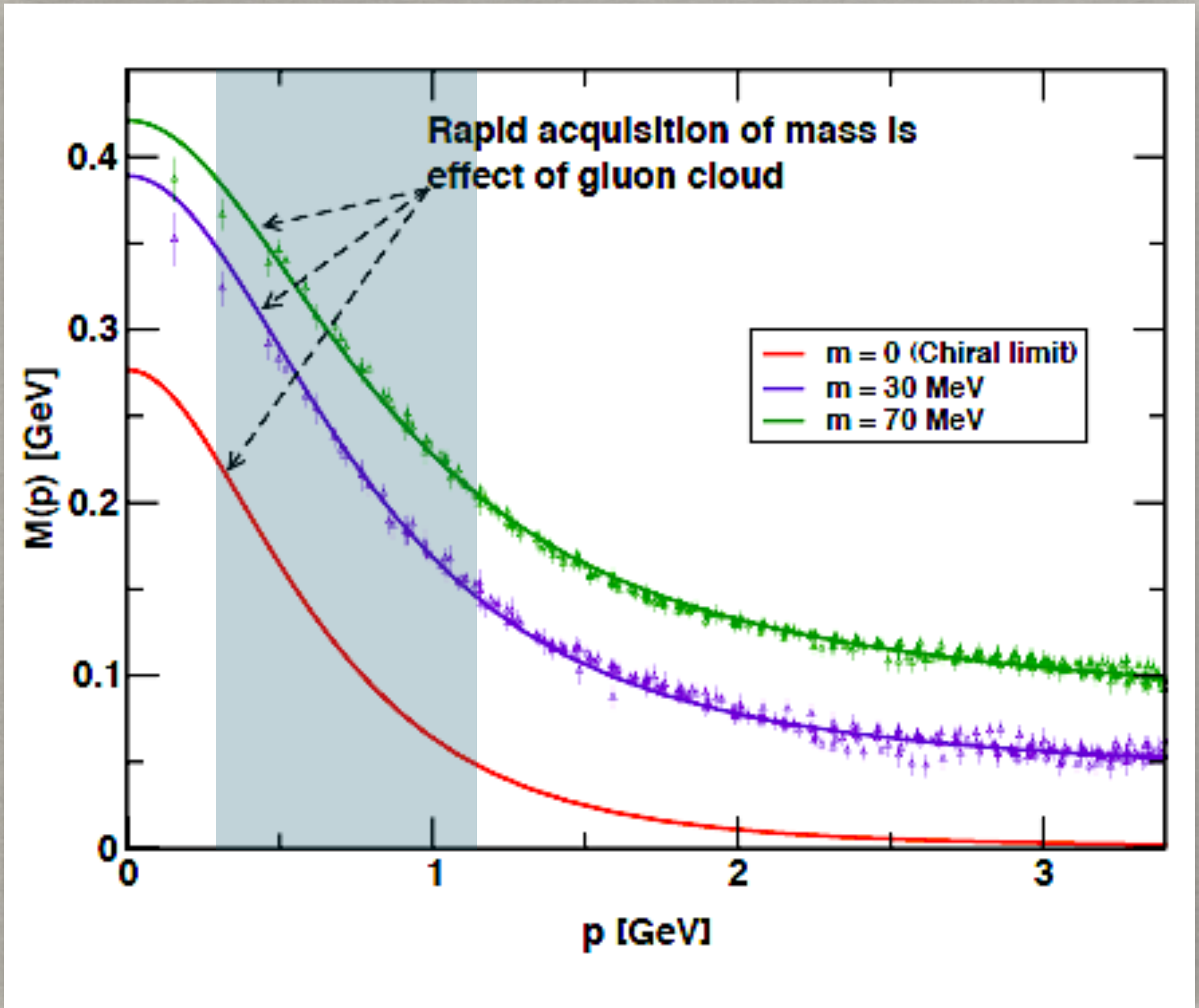

$$S(p) = \frac{Z(p^2)}{i\gamma \cdot p + M(p^2)}$$

➪ For light quarks the Higgs mechanism is almost irrelevant!

Motivation: Connection with Real World

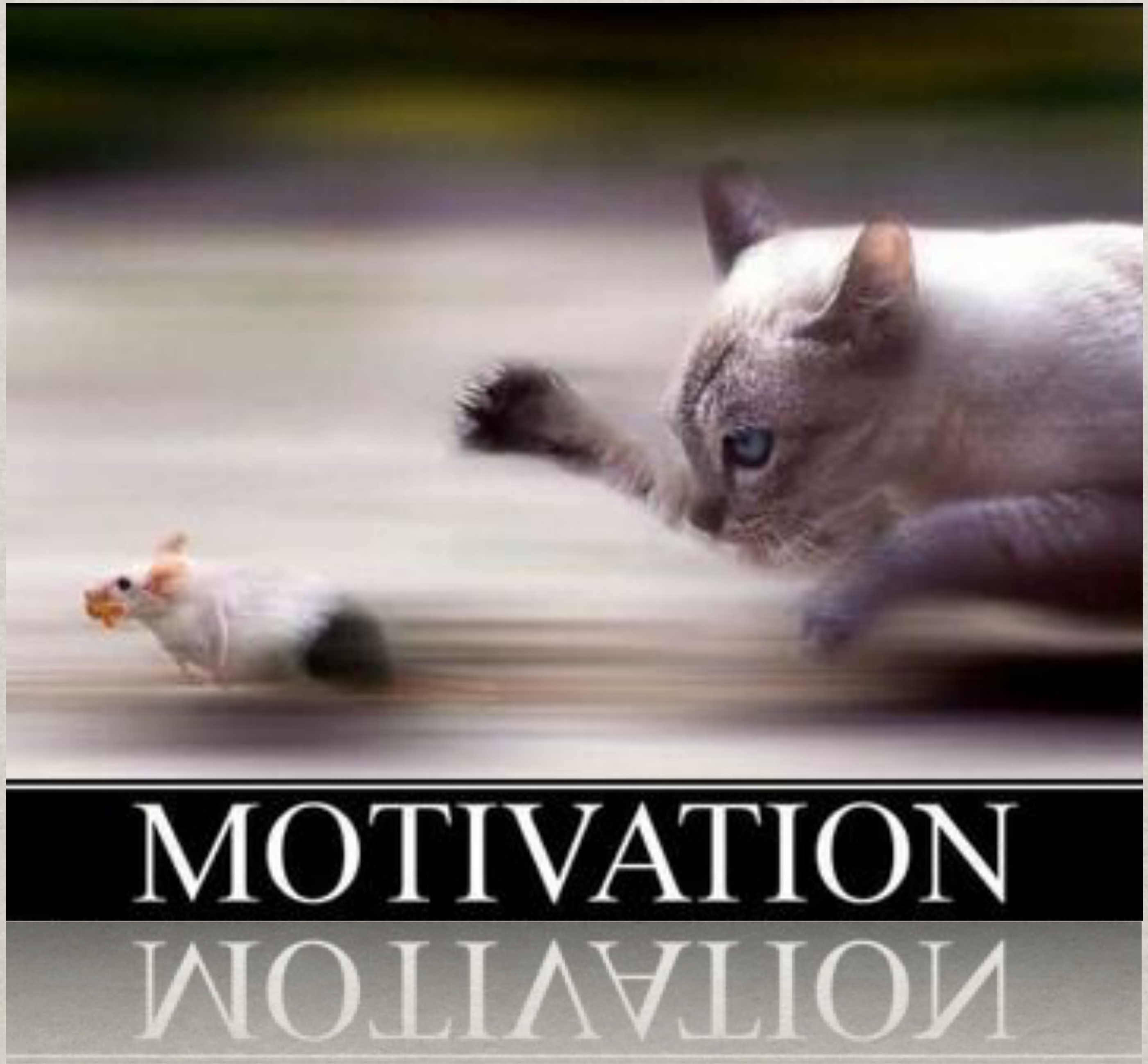

Motivation: Connection with Real World

- How does one incorporate the dressed-quark mass function $M(p^2)$ in study of mesons and baryons? The behavior of $M(p^2)$ is *a quantum field theoretical effect*.

- In quantum field theory a meson (nucleon) appears as a pole in the four (six)-point quark Green functions amplitude.

- Residue is proportional to meson's Bethe-Salpeter or nucleon's Faddeev amplitude.

- Poincaré covariant Bethe-Salpeter/Faddeev equation sum all possible exchanges and interactions that can take place between dressed-quarks ($Q^2 \gg M^2$).

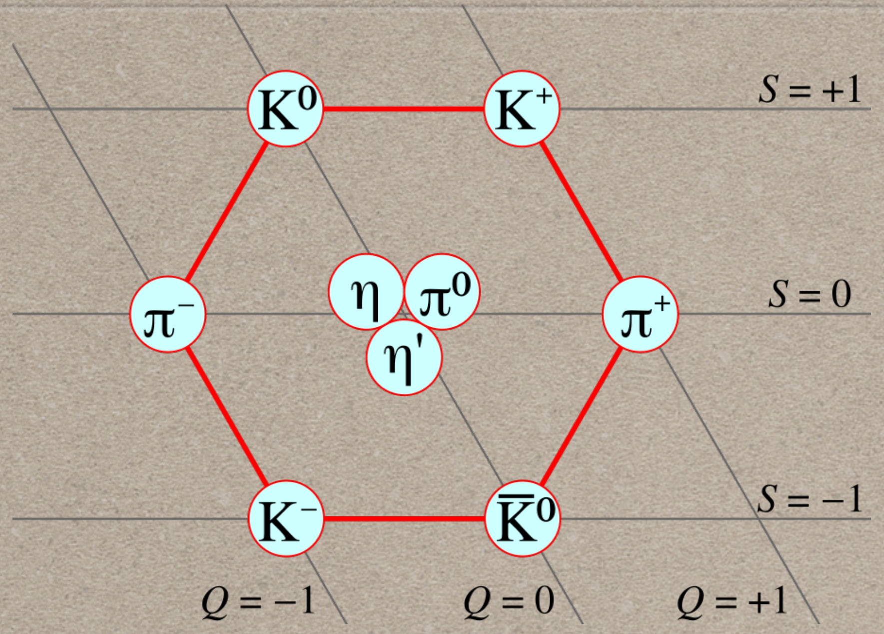

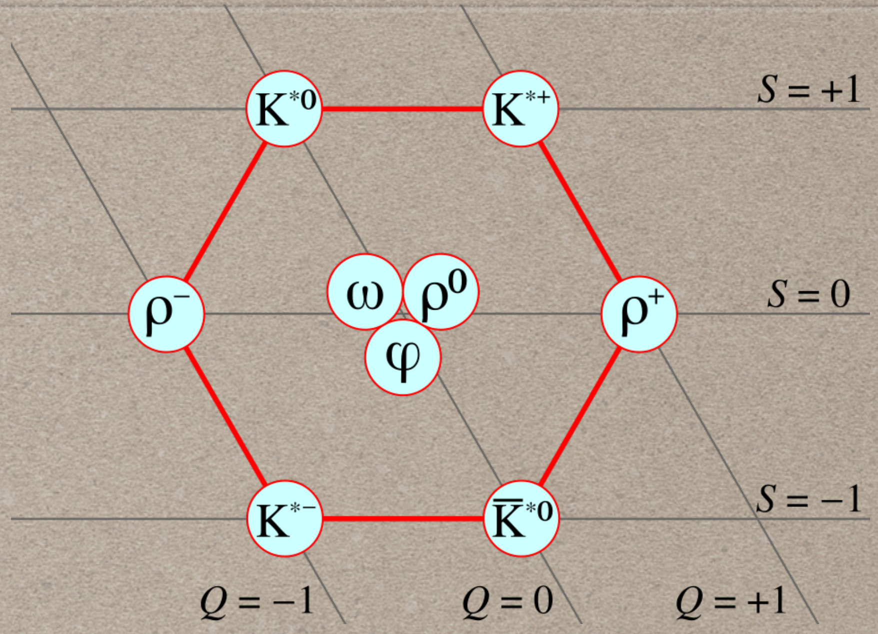

Meson Bound States

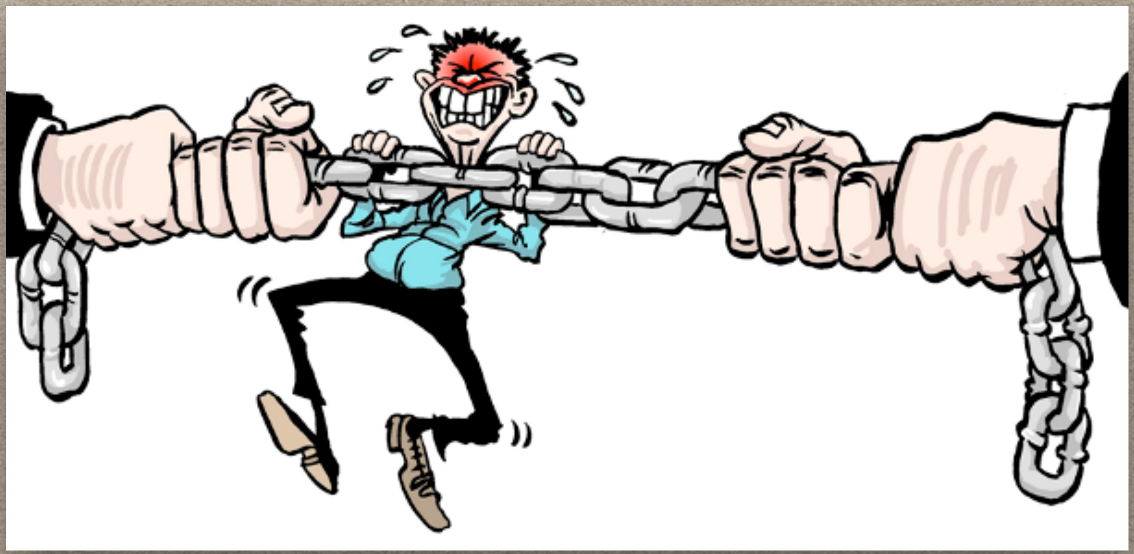

Bethe-Salpeter Equations for QCD Bound States

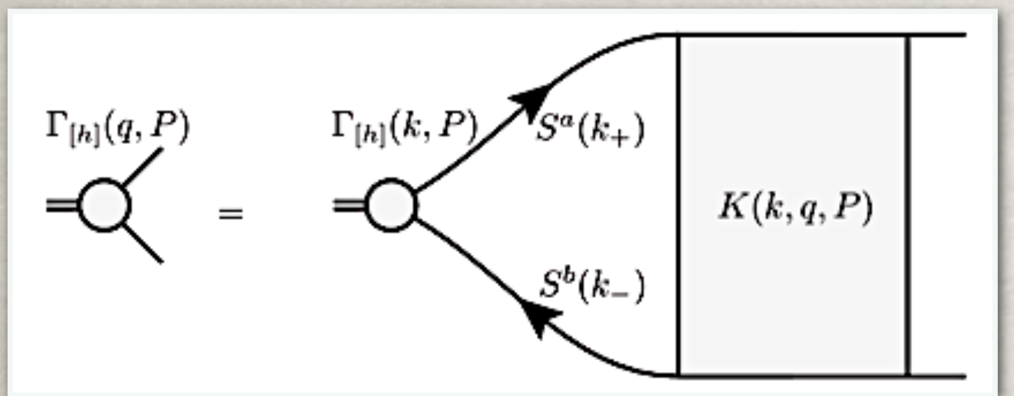

Nonperturbative QCD based ansatz for interaction kernel

$$\Gamma(P,p) = \int \frac{d^4k}{(2\pi)^4} K(P,p,k)\, S(k-\tfrac{P}{2})\, \Gamma(P,k)\, S(k+\tfrac{P}{2})$$

Rainbow-Ladder truncation:

$$K(P,p,k) = -\frac{Z_2^2\, \mathcal{G}(q^2)}{q^2} \left(\frac{\lambda^a}{2}\gamma_\mu\right) T_{\mu\nu}(q) \left(\frac{\lambda^a}{2}\gamma_\nu\right)$$

Rainbow-ladder truncation (leading symmetry-preserving approximation)

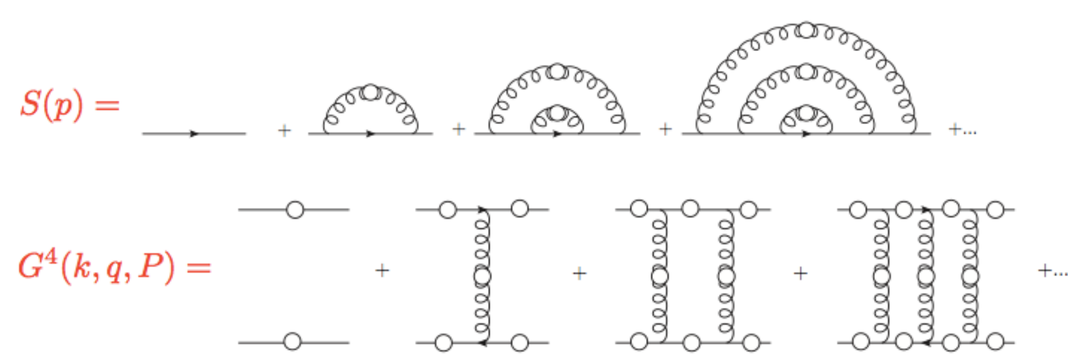

Model gluon propagator, solve quark propagator and 4-point Green function.

Bethe-Salpeter Equations for QCD Bound States

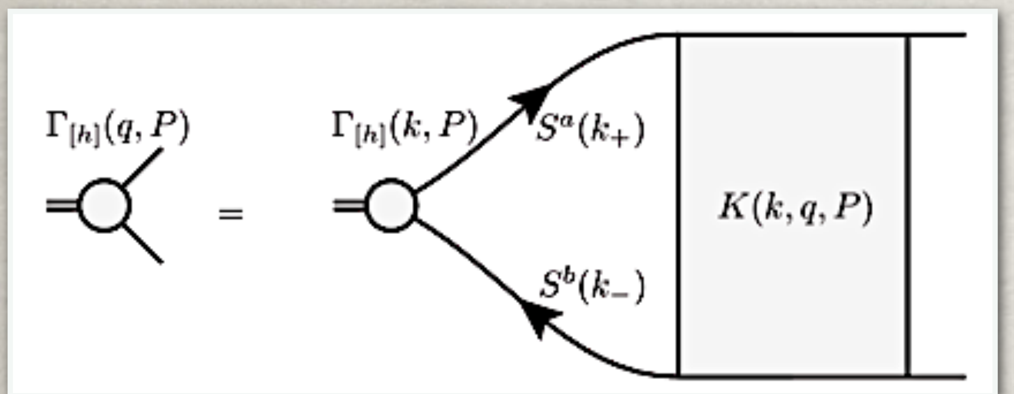

Nonperturbative QCD based ansatz for interaction kernel

$$\Gamma(P,p) = \int \frac{d^4k}{(2\pi)^4} K(P,p,k)\, S(k-\tfrac{P}{2})\,\Gamma(P,k)\, S(k+\tfrac{P}{2})$$

Rainbow-Ladder truncation:

$$K(P,p,k) = -\frac{Z_2^2\, \mathcal{G}(q^2)}{q^2}\left(\frac{\lambda^a}{2}\gamma_\mu\right) T_{\mu\nu}(q) \left(\frac{\lambda^a}{2}\gamma_\nu\right)$$

General solution for Poincaré invariant ground- and excited-state amplitudes

$$\begin{aligned}\Gamma_{P_n}(p,P) = \gamma_5 \big[\, i\,\mathbb{I}_D E_{P_n}(p,P) + \gamma\cdot P\, F_{P_n}(p,P) \\ + \gamma\cdot p\,(p\cdot P) G_{P_n}(p,P) + \sigma_{\mu\nu} p_\mu P_\nu\, H_{P_n}(p,P)\big]\end{aligned}$$

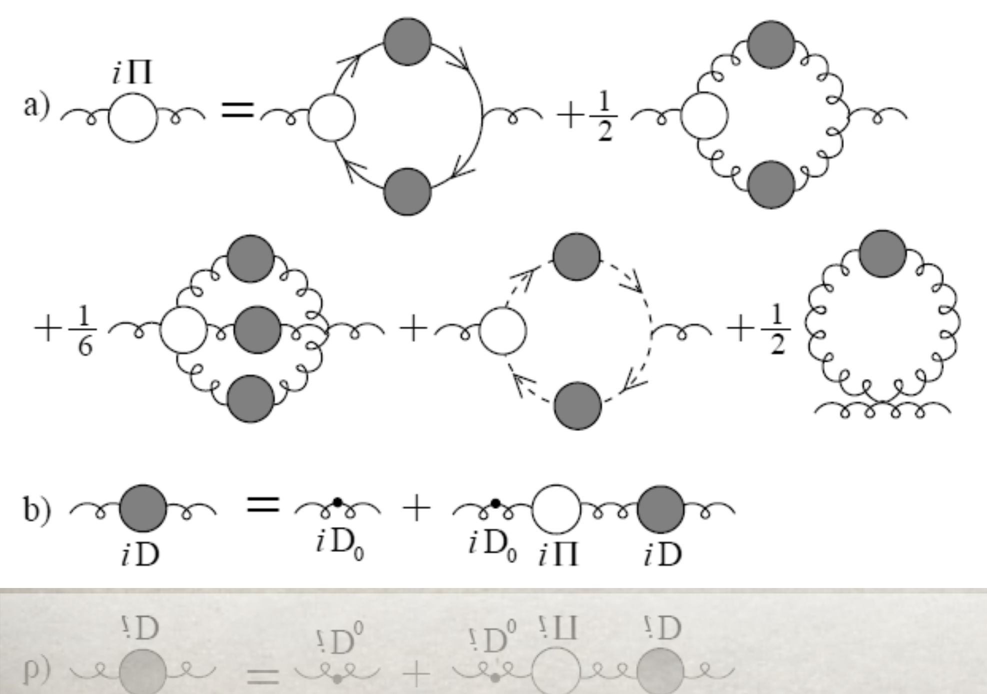

A.C. Aguilar et al., Phys.Rev. D80, 085018 (2009)

Dressed-gluon propagator

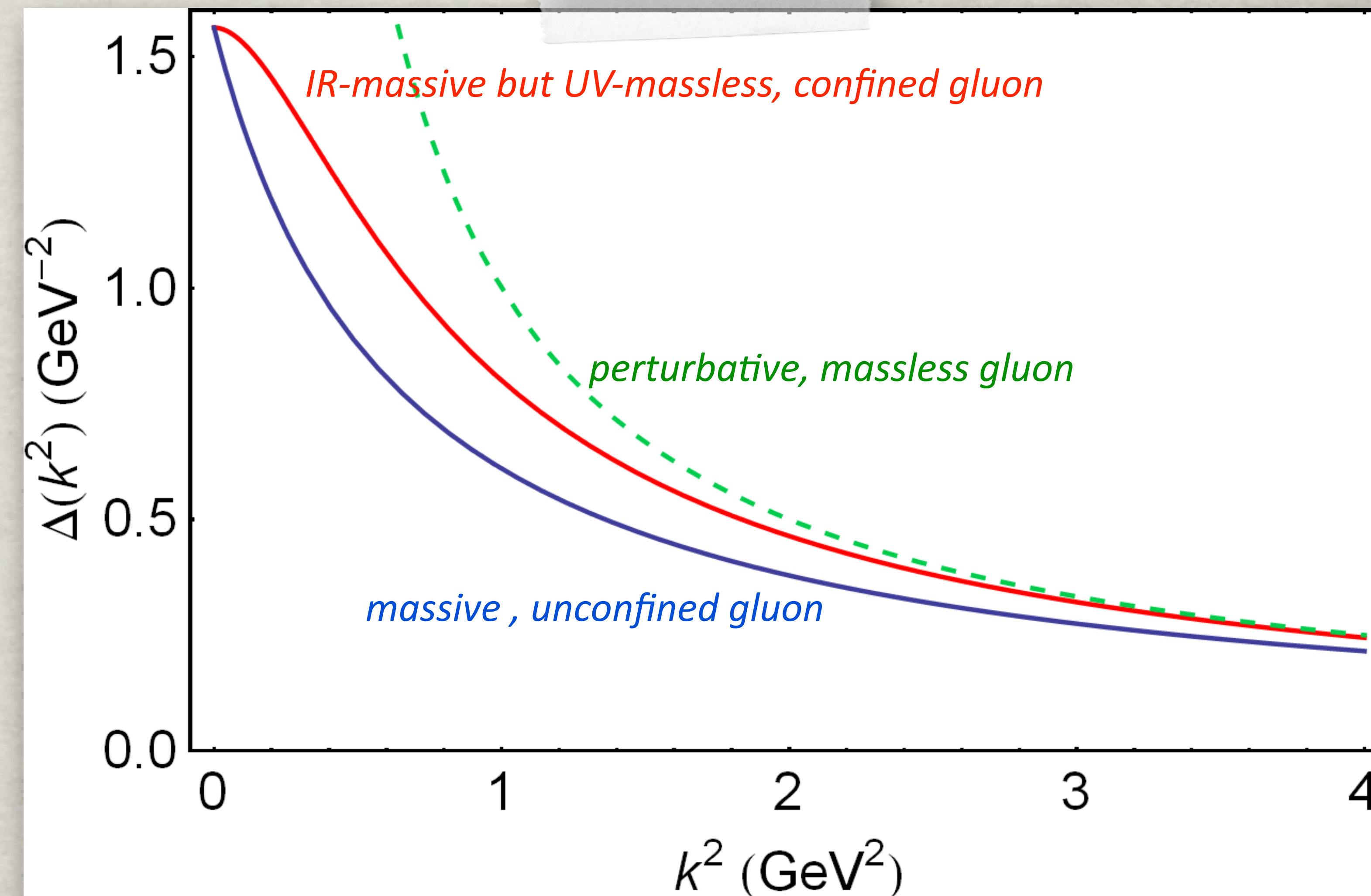

Use effective interaction which reproduces Lattice QCD and DSE results for gluon-dressing function: *infrared massive fixed point; ultraviolet massless propagator.*

$$\Delta(k^2) \approx \frac{4\pi\alpha(k^2)}{k^2 + m_g^2(k^2)}, \quad m_g^2(k^2) = \frac{M_g^4}{M_g^2 + k^2}$$

Qin, Chang, Liu, Roberts and Wilson 2011

$$\mathcal{G}(s) = \frac{8\pi^2}{\omega^4} D e^{-s/\omega^2} + \frac{8\pi^2 \gamma_m}{\ln\left[\tau + (1 + s/\Lambda_{QCD}^2)\right]} \mathcal{F}(s)$$

Pseudoscalar- and Vector-Meson Spectroscopy

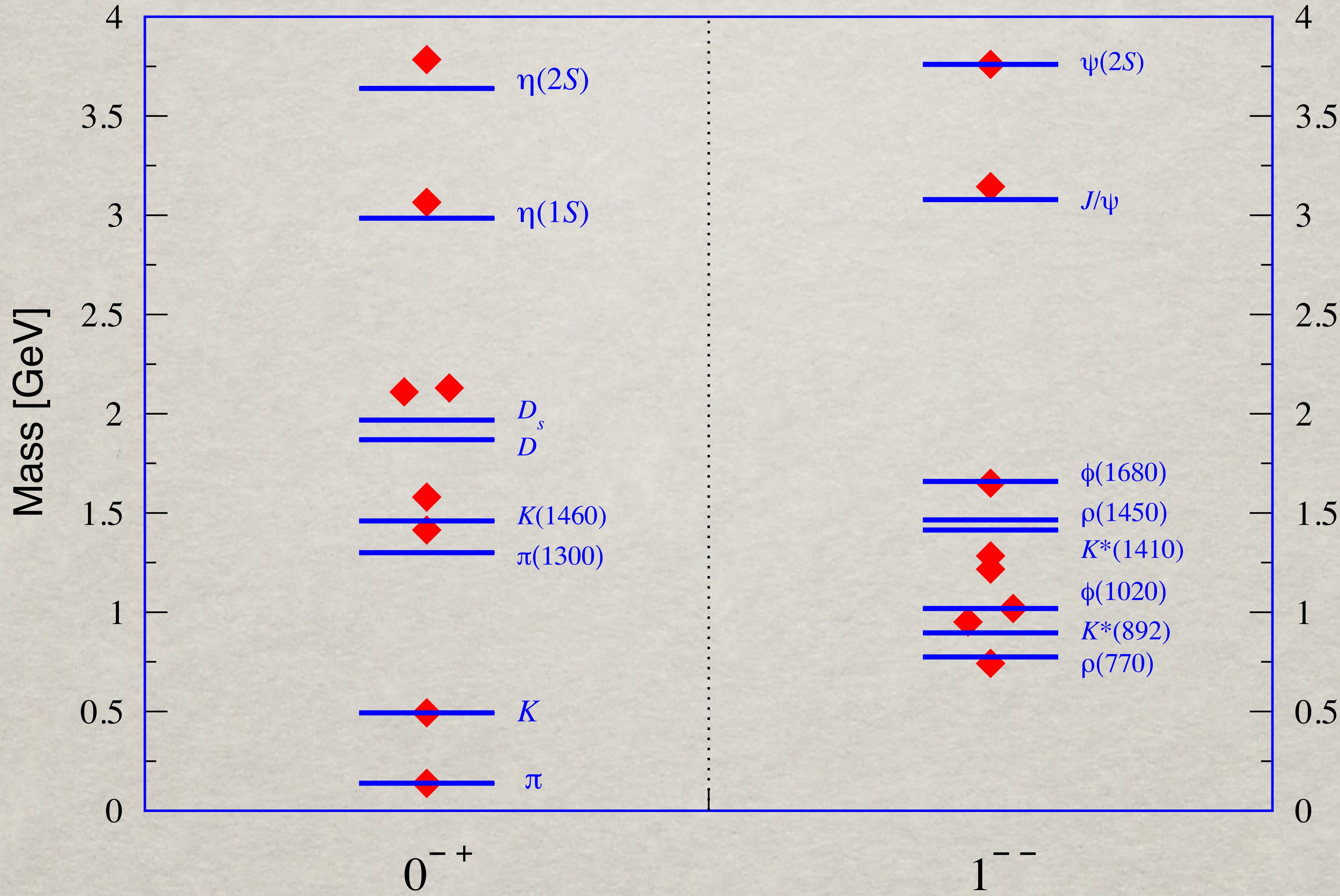

E. Rojas, B. E. & J. P. B. C. de Melo, PRD (2014)

F. Mojica, C. Vera, E. Rojas & B. E., PRD (2017)

Bethe-Salpeter Equations as an Eigenvalue Problem

$$\lambda(P^2)\,\Gamma_{P_n}(P,p) = \int \frac{d^4k}{(2\pi)^4}\, K(P,p,k)\,\chi_{P_n}(k,P)$$

$$\chi_{P_n}(k,P) = S(k-\tfrac{P}{2})\,\Gamma(P,k)\,S(k+\tfrac{P}{2}) \; : \; \text{Bethe-Salpeter wave function}$$

The kernel $\mathcal{K}(P^2)$ has a complete set of real eigenvectors ϕ_i with eigenvalues $\lambda_i(P^2)$ which are ordered as $\lambda_0(P^2) > \lambda_1(P^2) > \lambda_2(P^2) > .... > \lambda_i(P^2)$.

$$\lambda(P^2)\,|\Phi\rangle = \mathcal{K}(P^2)\,|\Phi\rangle \longrightarrow |\Phi\rangle = \sum_{i=1}^{\infty} a_i\,|\,\phi_i\rangle$$

$$|\,\phi_n\rangle := \mathcal{K}^n(P^2)\,|\Phi\rangle = \sum_{i=1}^{\infty} \lambda_i^n a_i\,|\,\phi_i\rangle = \lambda_0^n\left[a_0\,|\,\phi_0\rangle + \sum_{i=1}^{\infty}\left(\frac{\lambda_i}{\lambda_0}\right)^n a_i\,|\,\phi_i\rangle\right]$$

$$|\,\phi_n\rangle \overset{n\to\infty}{=} \lambda_0^n\, a_0\,|\,\phi_0\rangle \simeq \lambda_0\,\mathcal{K}^{n-1}(P^2)\,|\Phi\rangle$$

B. El-Bennich & E. Rojas arXiv:1509.02919 (2015)

- Eigenvalue spectrum is not limited to the ground state.
- Excited states with smaller eigenvalues can be determined with the same iterative methods.
- Usage of Gram-Schmidt orthogonalization process:

$$|\tilde{\Phi}\rangle = |\Phi\rangle - \frac{\langle \phi_0 \,|\, \Phi \rangle}{\langle \phi_0 \,|\, \phi_0 \rangle} \, |\phi_0\rangle$$

- Eigenvalue spectrum is not limited to the ground state.
- Excited states with smaller eigenvalues can be determined with the same iterative methods.
- Usage of Gram-Schmidt orthogonalization process:

$$|\tilde{\Phi}\rangle = |\Phi\rangle - \frac{\langle \phi_0 \,|\, \Phi \rangle}{\langle \phi_0 \,|\, \phi_0 \rangle}\, |\phi_0\rangle$$

- Modern and more efficient approach is the implicitly restarted Arnoldi method (IRAM).
- Based on the stabilized Gram-Schmidt orthogonalization in the Krylov subspace obtained by iteration:

$$\mathcal{S}_r \;:=\; \left\{ \Phi, K\Phi, K^2\Phi, K^3\Phi, ..., K^{r-1}\Phi \right\}$$

- Eigenvalue spectrum is not limited to the ground state.
- Excited states with smaller eigenvalues can be determined with the same iterative methods.
- Usage of Gram-Schmidt orthogonalization process:

$$|\tilde{\Phi}\rangle = |\Phi\rangle - \frac{\langle \phi_0 \,|\, \Phi \rangle}{\langle \phi_0 \,|\, \phi_0 \rangle} \, |\phi_0\rangle$$

- Modern and more efficient approach is the implicitly restarted Arnoldi method (IRAM).
- Based on the stabilized Gram-Schmidt orthogonalization in the Krylov subspace obtained by iteration:

$$\mathcal{S}_r \;:=\; \left\{ \Phi, K\Phi, K^2\Phi, K^3\Phi, ..., K^{r-1}\Phi \right\}$$

- The Arnoldi method generalizes the Gram-Schmidt process by computing the eigenvalues of the orthogonal projection of ***K*** onto the Krylov subspace $\Rightarrow$ yields smaller eigenvalues.

Examples of eigenvalue spectrum: pion ground and radially excited states

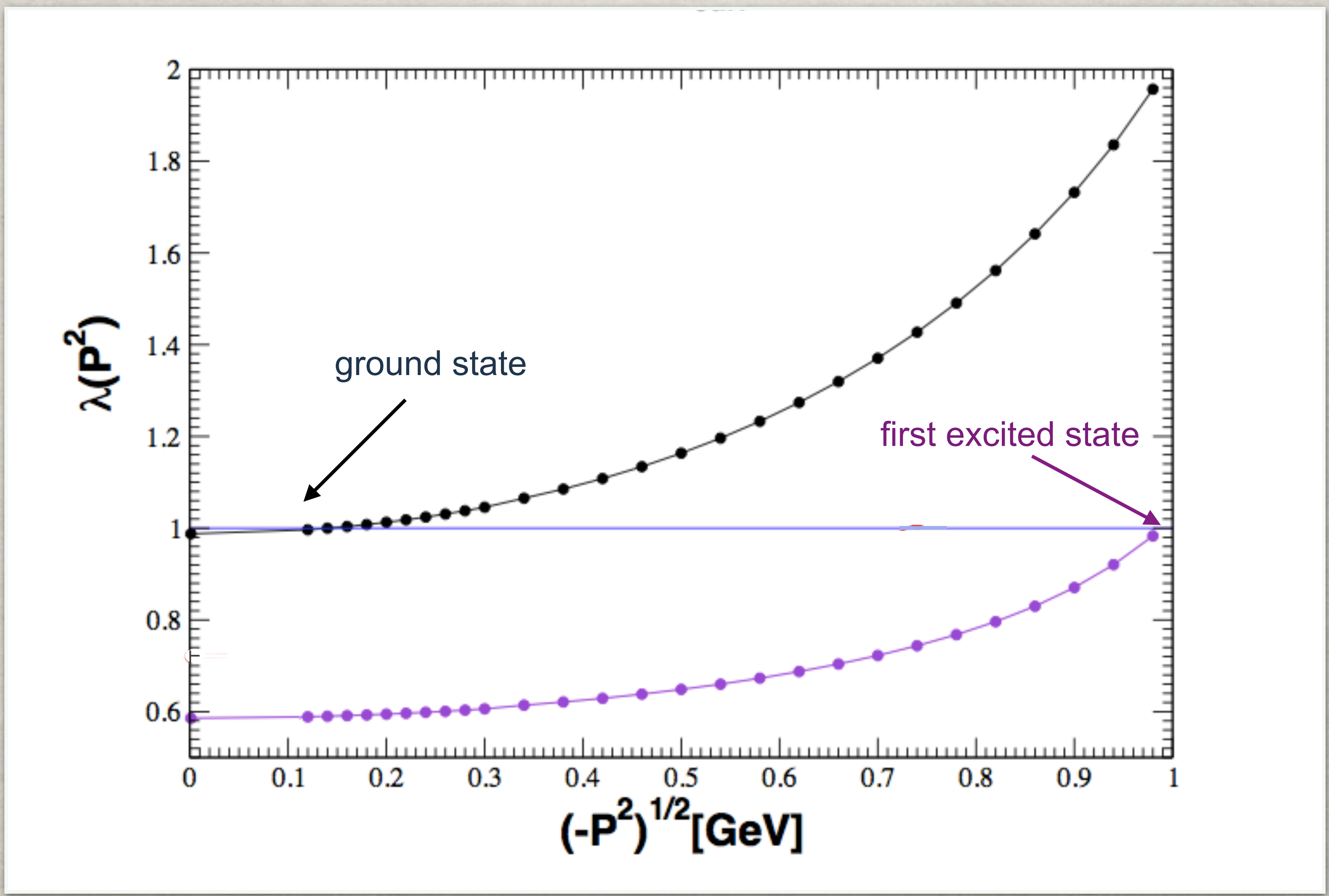

Chebyshev expansion of 1st excited state: $E_{P_1}(p,P) = \sum_{m=0}^{\infty} E^m_{P_1}(p,P)\, U_m(\cos\theta)$

$$\Gamma_{P_n}(p,P) = \gamma_5 \big[\, i\, \mathbb{I}_D E_{P_n}(p,P) + \gamma\cdot P\, F_{P_n}(p,P) + \gamma\cdot p\,(p\cdot P) G_{P_n}(p,P) + \sigma_{\mu\nu} p_\mu P_\nu\, H_{P_n}(p,P) \big]$$

Lowest Chebyshev moment : $E^0_{P_1}(p^2, P^2)$

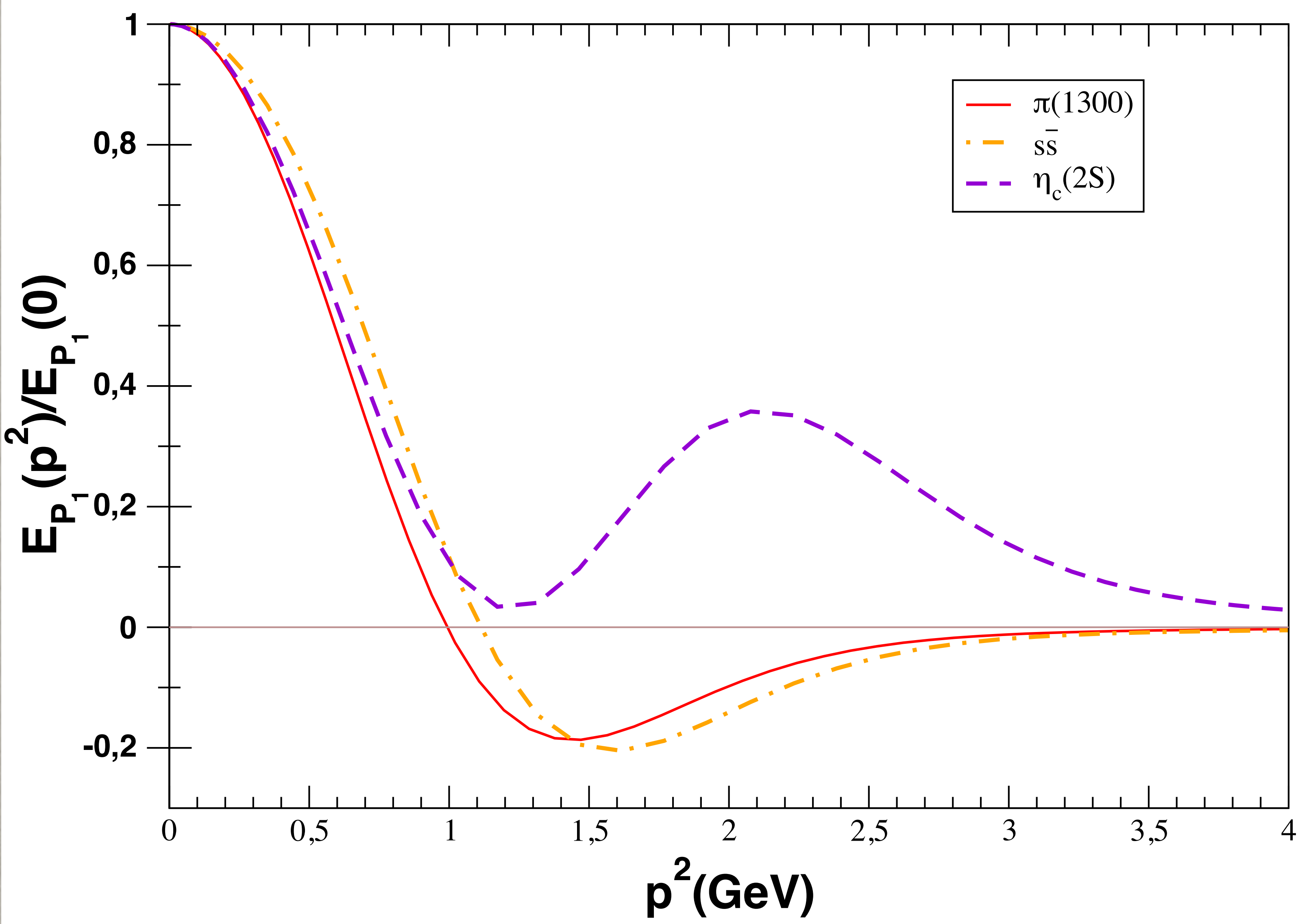

Pseudoscalar- and Vector-Meson Spectroscopy

$J^{PC} = 0^{-+}$	DSE-BSE	PDG
m_π	0.136	0.139
f_π	0.139	0.1304
$m_{\pi(1300)}$	1.414	1.30 ± 0.10
$f_{\pi(1300)}$	8.3×10^{-4}	—
m_K	0.493	0.493
f_K	0.164	0.156
$m_{K(1460)}$	1.580	1.460
$f_{K(1460)}$	0.017	—
$m_{\eta_c(1S)}$	3.065	2.984
$f_{\eta_c(1S)}$	0.389	0.395
$m_{\eta_c(2S)}$	3.784	3.639
$f_{\eta_c(2S)}$	0.105	—

E. Rojas, B. E. & J. P. B. C. de Melo, PRD (2014)
F. Mojica, C. Vera, E. Rojas & B. E., PRD (2017)

Weak decay constant for radially excited states vanish — only strong decays possible:

$$f^0_{P_n} \equiv 0\,, \;\; n \geq 1$$

$J^{PC} = 1^{--}$	DSE-BSE	PDG
$m_{\rho^0(770)}$	0.742	0.775
$f_{\rho^0(770)}$	0.231	0.221
$m_{\rho^0(1450)}$	1.284	1.465
$f_{\rho^0(1450)}$	0.150	—
$m_{K^*(892)}$	0.951	0.896
$f_{K^*(892)}$	0.287	0.217
$m_{K^*(1410)}$	1.217	1.414
$f_{K^*(1410)}$	0.127	—
$m_{\phi(1020)}$	1.087	1.019
$f_{\phi(1020)}$	0.305	0.322
$m_{\phi(1680)}$	1.650	1.659
$f_{\phi(1680)}$	0.138	—
$m_{J/\psi}$	3.114	3.097
$f_{J/\psi}$	0.433	0.416
$m_{\psi(2S)}$	3.760	3.689
$f_{\psi(2S)}$	0.176	0.295
$m_{\Upsilon(1S)}$	9.634	9.460
$f_{\Upsilon(1S)}$	—	0.715
$m_{\Upsilon(2S)}$	10.140	10.023
$f_{\Upsilon(2S)}$	0.564	0.497

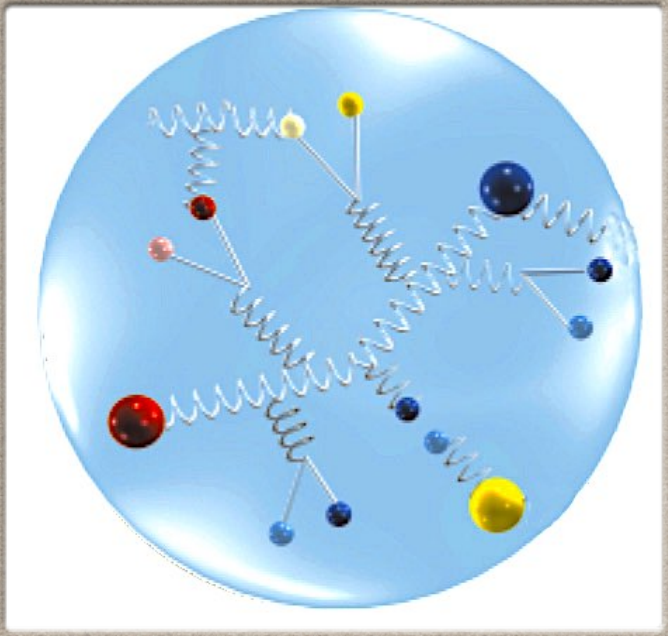

Baryon Spectrum

SU(3): $3 \otimes 3 = \bar{3} \oplus 6$

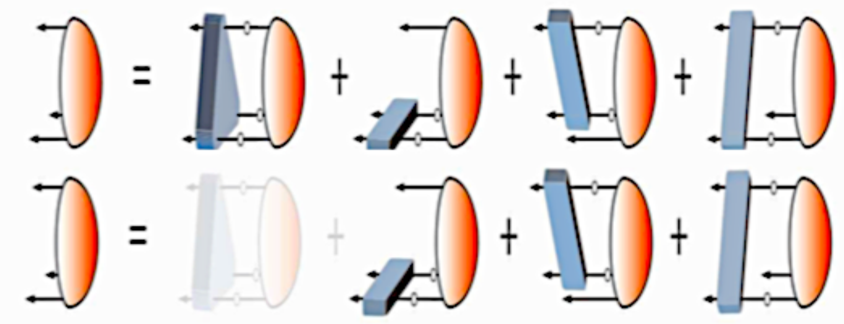

Thanks to G. Eichmann.

Covariant Fadeev Equation

- The attractive nature of quark-antiquark correlations in a color-singlet meson is also attractive for $\bar{3}_c$ quark-quark correlations within a color-singlet baryon.

- *Diquark correlations* provide a tractable truncation of the Faddeev equation.

- We use non-pointlike color-antitriplet and fully interacting *diquarks* in the description of the Baryon Octet and Decuplet.

- Scalar and axialvector diquarks: dominant right parity.

SU(3): $3 \otimes 3 = \bar{3} \oplus 6$

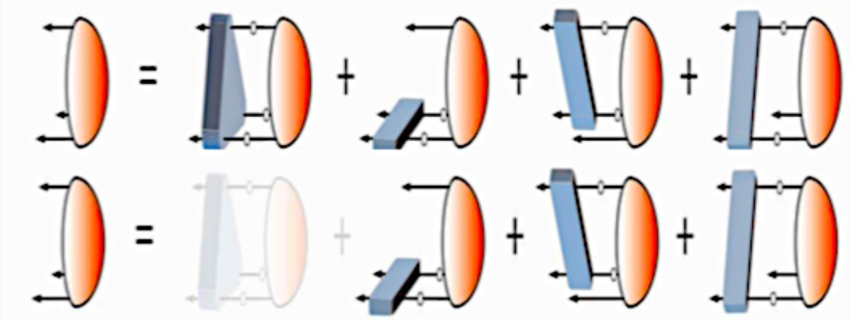

Covariant Fadeev Equation

- The attractive nature of quark-antiquark correlations in a color-singlet meson is also attractive for $\bar{3}_c$ quark-quark correlations within a color-singlet baryon.
- *Diquark correlations* provide a tractable truncation of the Faddeev equation.
- We use non-pointlike color-antitriplet and fully interacting *diquarks* in the description of the Baryon Octet and Decuplet.
- Scalar and axialvector diquarks: dominant right parity.
- Typically, $r_{0+} \sim r_\pi$ & $r_{1+} \sim r_\rho$ (actually 10% larger).
- Pseudoscalar and vector diquarks: initially neglected, **now included**.
- Diquarks: have soft form factors.

Covariant Fadeev Equation

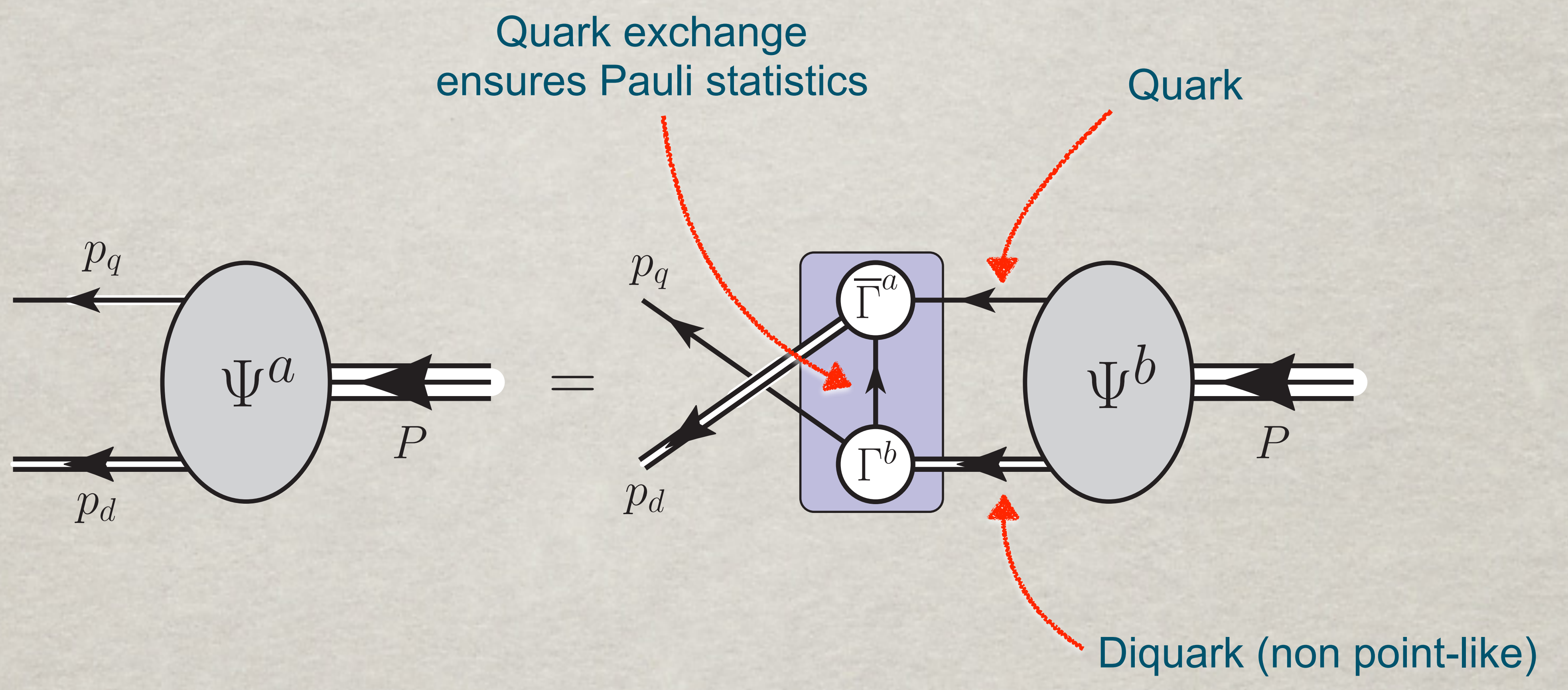

R.T. Cahill, C.D. Roberts, J. Praschifka (1989)

M. Oettel, L. von Smekal, R. Alkofer (2001)

I.C. Cloët, G. Eichmann, B. El-Bennich, T. Klähn and C.D. Roberts (2009)

G. Eichmann, C. Fischer, H. Sanchis-Alepuz (2016)

Linear homogeneous matrix equation yields Poincaré covariant Faddeev amplitude (wave function) that describes relative motion of quark-diquark within nucleon.

Nucleon Electromagnetic Form Factors

- Composite nucleon must interact with photon via nontrivial current constrained by Ward-Takahashi identities (EM gauge invariance).
- Coupling of the photon to the dressed quark.
- Coupling of the photon to the dressed diquark:
  Elastic & induced transitions
- Exchange and seagull terms.

$$J_\mu(P',P) = ie\,\bar{u}(P')\,\Lambda_\mu(q,P)\,u(P)\,,$$
$$= ie\,\bar{u}(P')\left(\gamma_\mu F_1(Q^2) + \frac{1}{2M}\,\sigma_{\mu\nu}\,Q_\nu\,F_2(Q^2)\right)u(P)$$

$$G_E(Q^2) = F_1(Q^2) - \frac{Q^2}{4M^2}F_2(Q^2)\,,\; G_M(Q^2) = F_1(Q^2) + F_2(Q^2)\,.$$

$$\mu_n = \kappa_n = G_M^n(0)\,,\;\mu_p = 1 + \kappa_p = G_M^p(0)$$

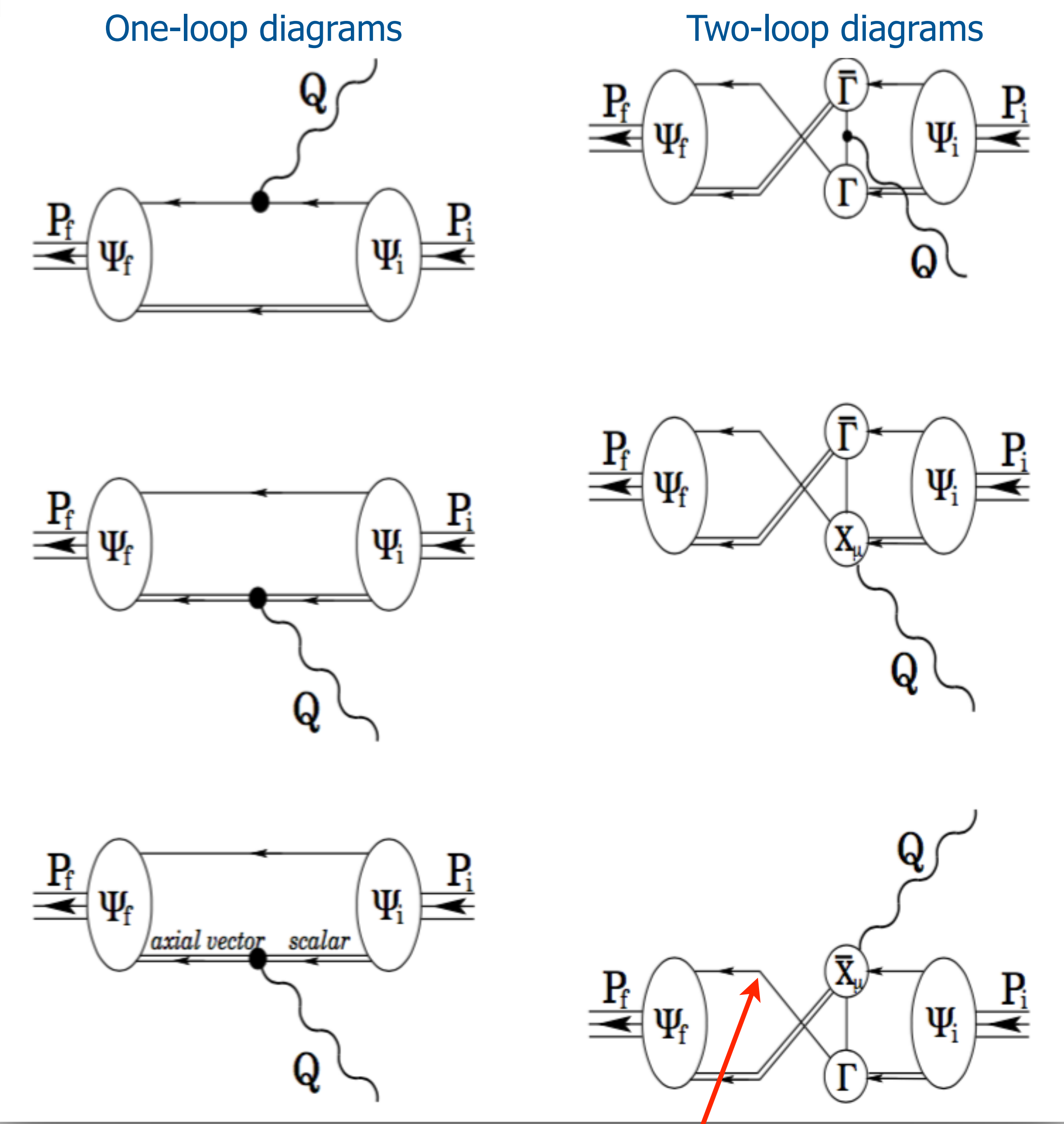

$$S(p) = -i\gamma\cdot p\,\sigma_V(p^2,\zeta^2) + \sigma_S(p^2,\zeta^2) = \frac{1}{i\gamma\cdot p\,A(p^2,\zeta^2) + B(p^2,\zeta^2)} = \frac{Z(p^2,\zeta^2)}{i\gamma\cdot p + M(p^2)}$$

Dressed quark propagator solutions of QCD's Dyson-Schwinger equations.

⇒ momentum dependence !

Proton's Sachs Electric and Magnetic Form Factors

$$G_E(Q^2) = F_1(Q^2) - \frac{Q^2}{4M^2} F_2(Q^2)\,,\; G_M(Q^2) = F_1(Q^2) + F_2(Q^2)$$

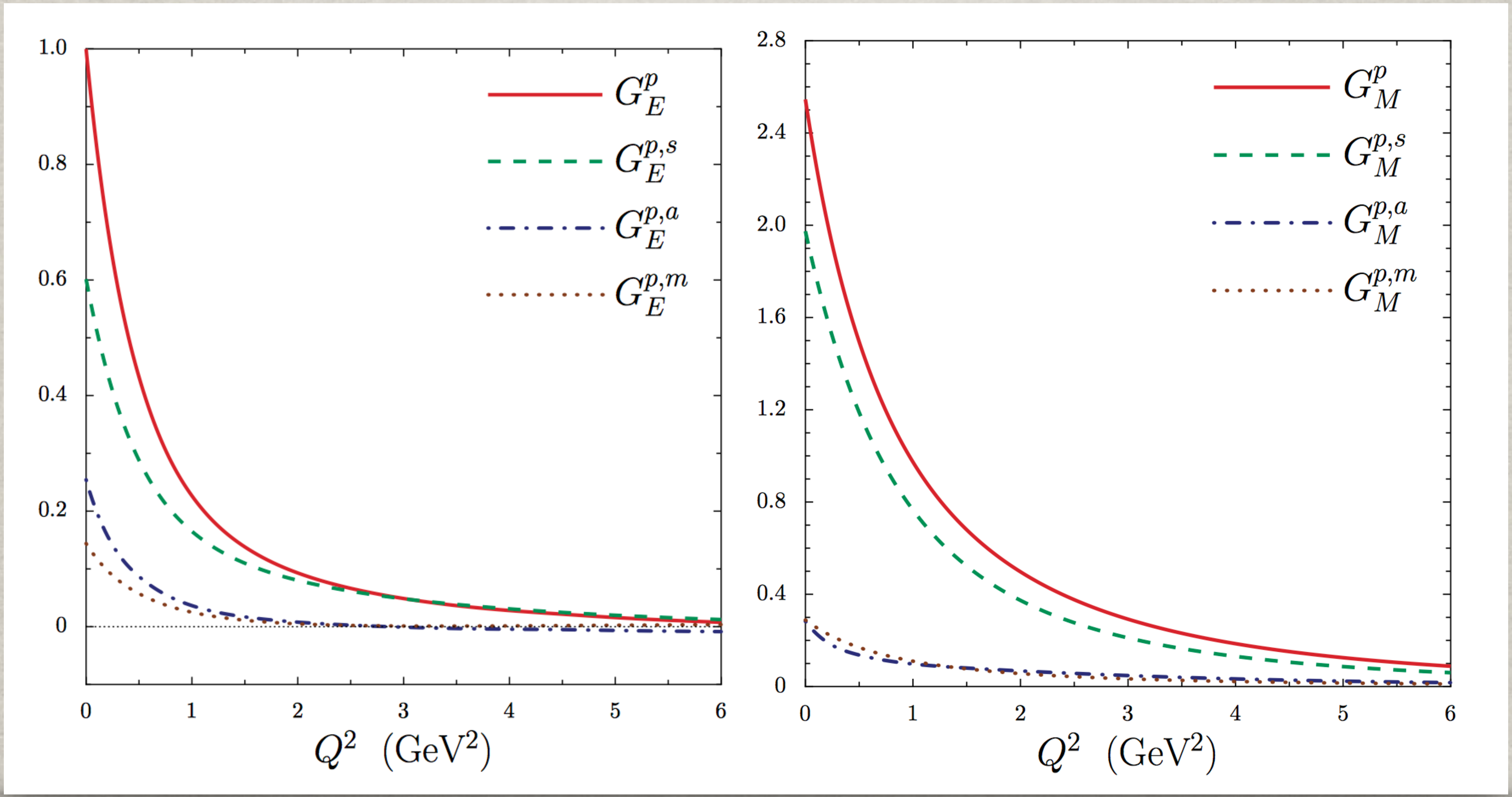

I.C. Cloët, G. Eichmann, B. El-Bennich, T. Klähn and C.D. Roberts, Few Body Syst. 46 (2009)

Electric Sachs form factors: mass function dependence

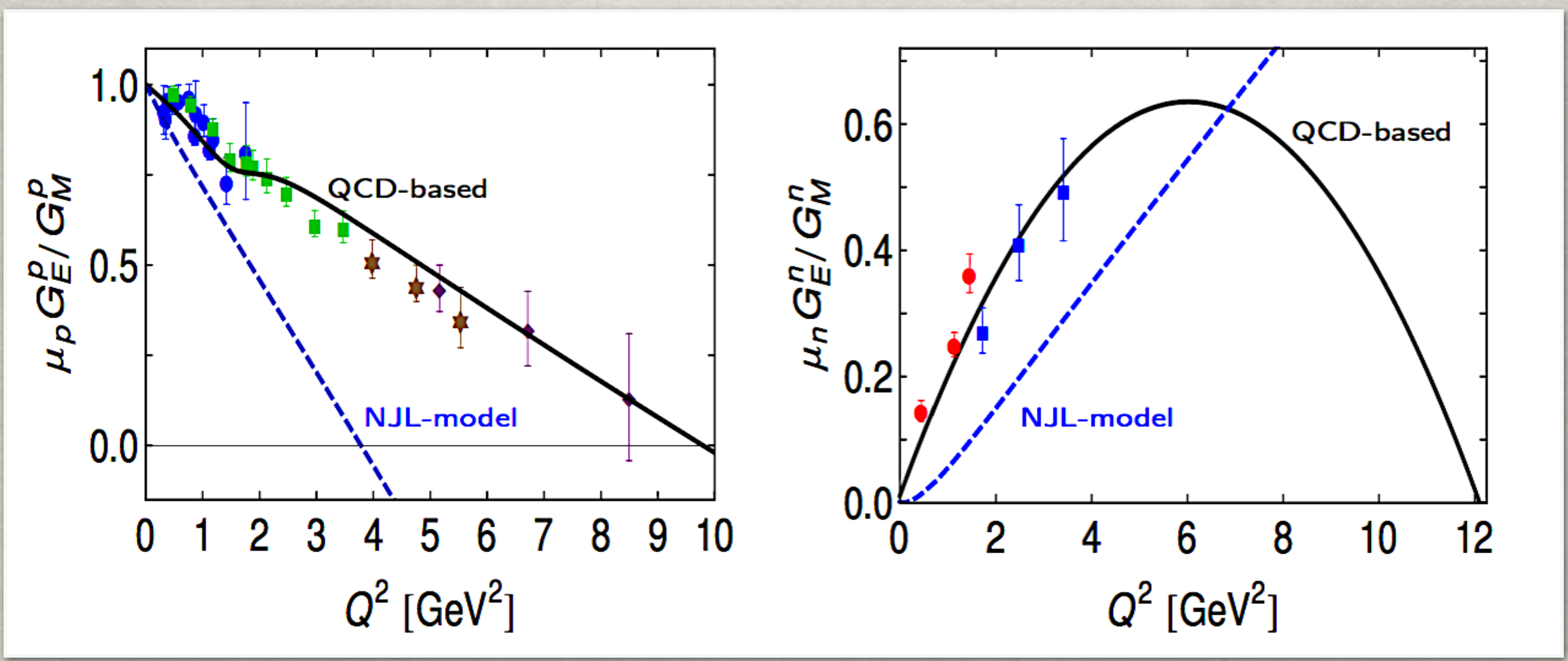

- Both CI and QCD-based frameworks predict a zero crossing in $\mu_p \frac{G_E^p}{G_M^p}$.
- The possible existence and location of the zero in $\mu_p \frac{G_E^p}{G_M^p}$ is an indirect measure of the nature of the quark-quark interaction.

A world with only scalar diquarks

The singly-represented d-quark in the proton $\equiv u[ud]_{0^+}$ *is sequestered inside a soft scalar diquark correlation.*

Contributions coming from **u-quark**

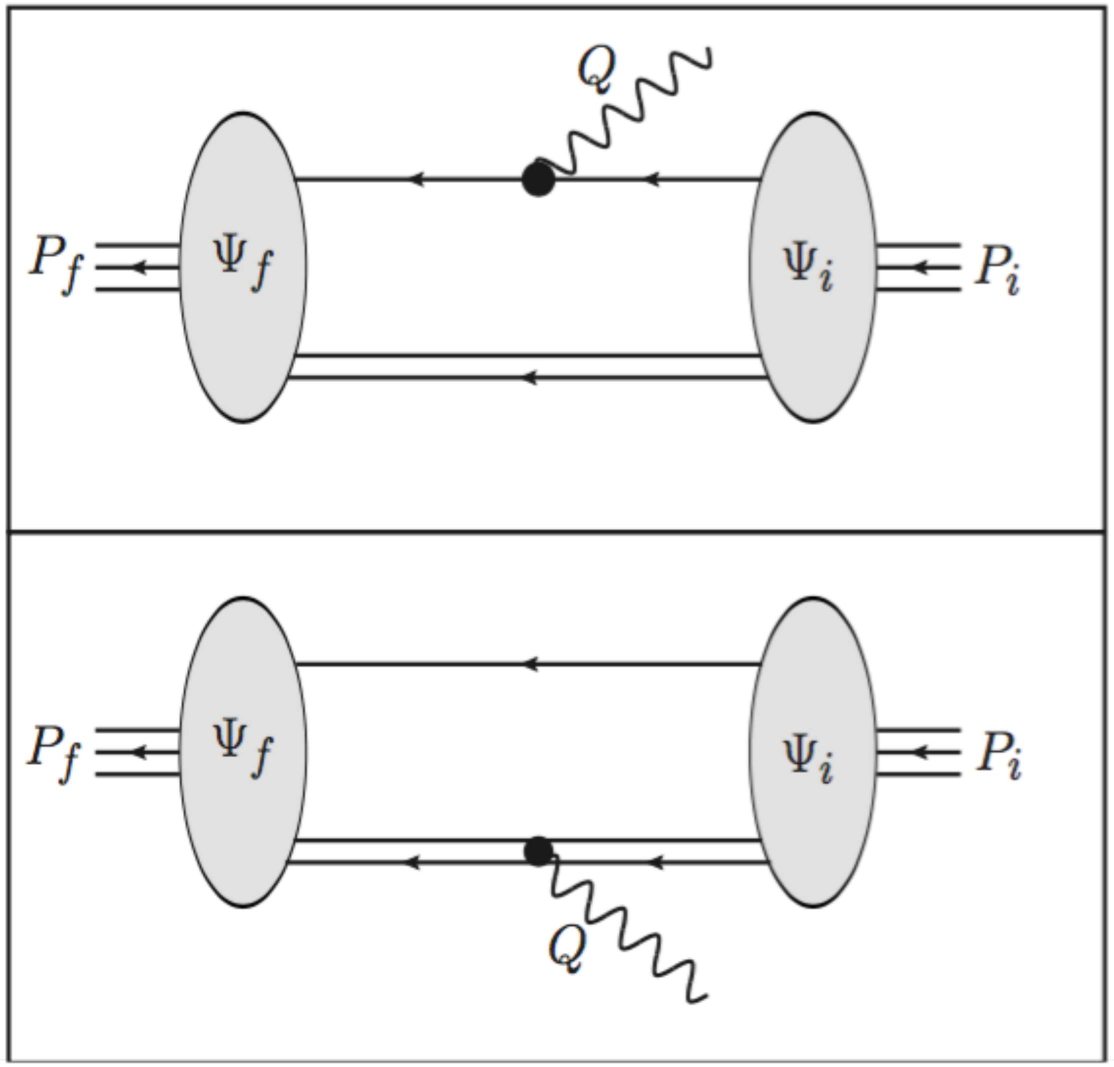

Contributions coming from **d-quark**

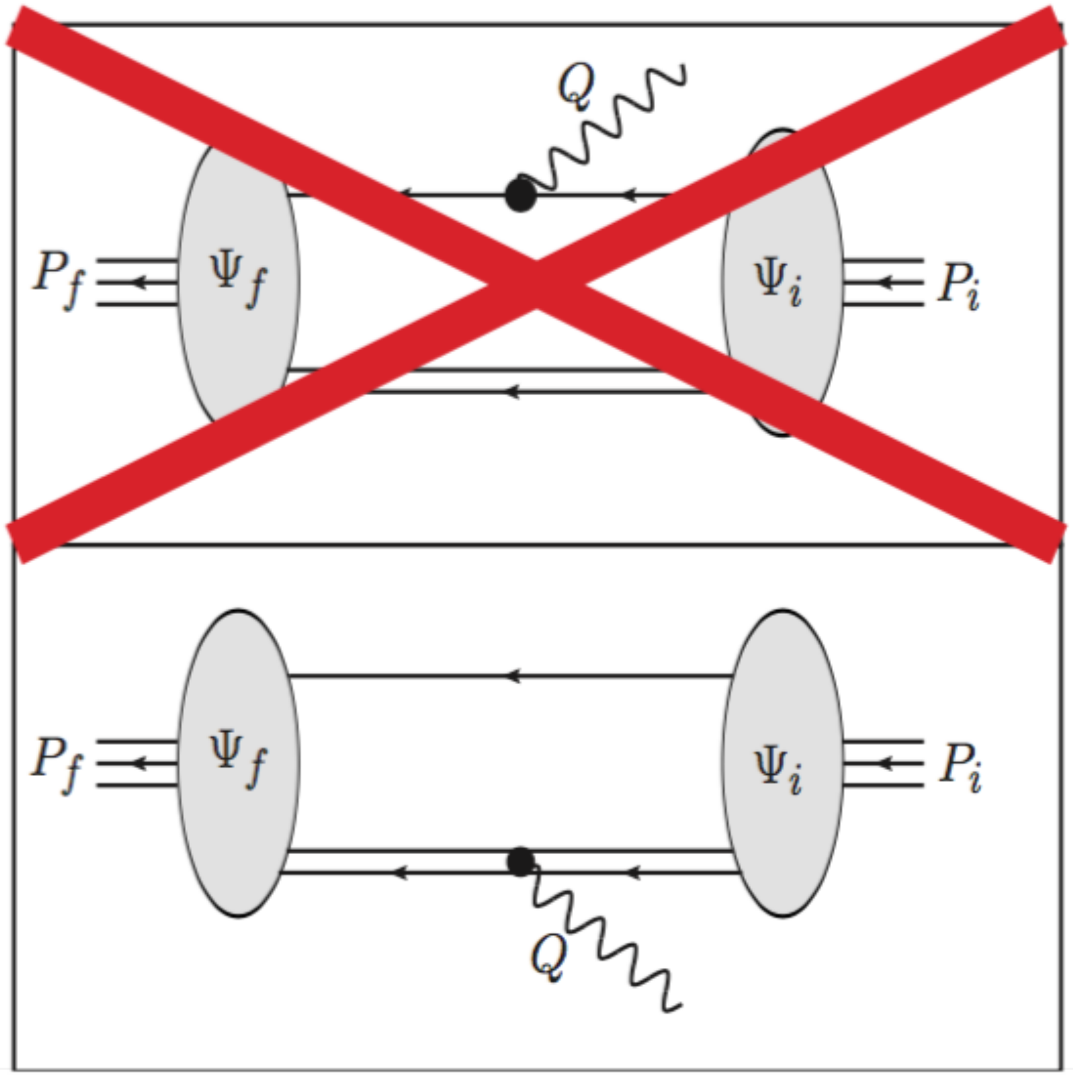

A world with scalar and axialvector diquarks

The singly-represented d-quark in the proton is **not always (but often)** *sequestered inside a soft scalar diquark correlation.*

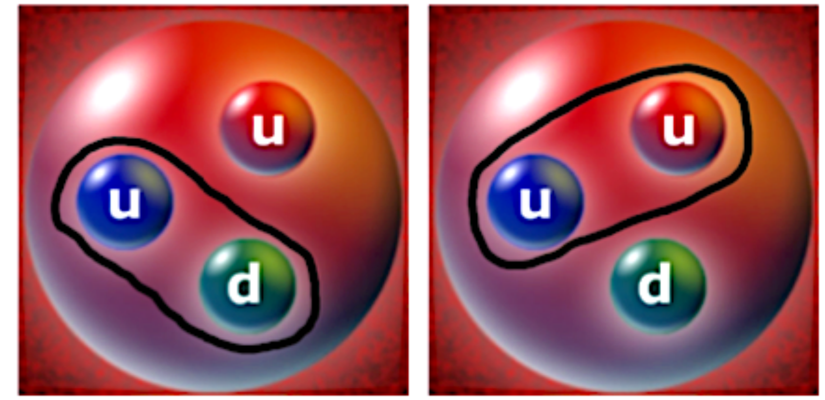

☞ *Observation:*

$$\mathcal{P}_{\text{scalar}} \sim 0.62, \quad \mathcal{P}_{\text{axial}} \sim 0.38$$

Contributions coming from **u-quark**

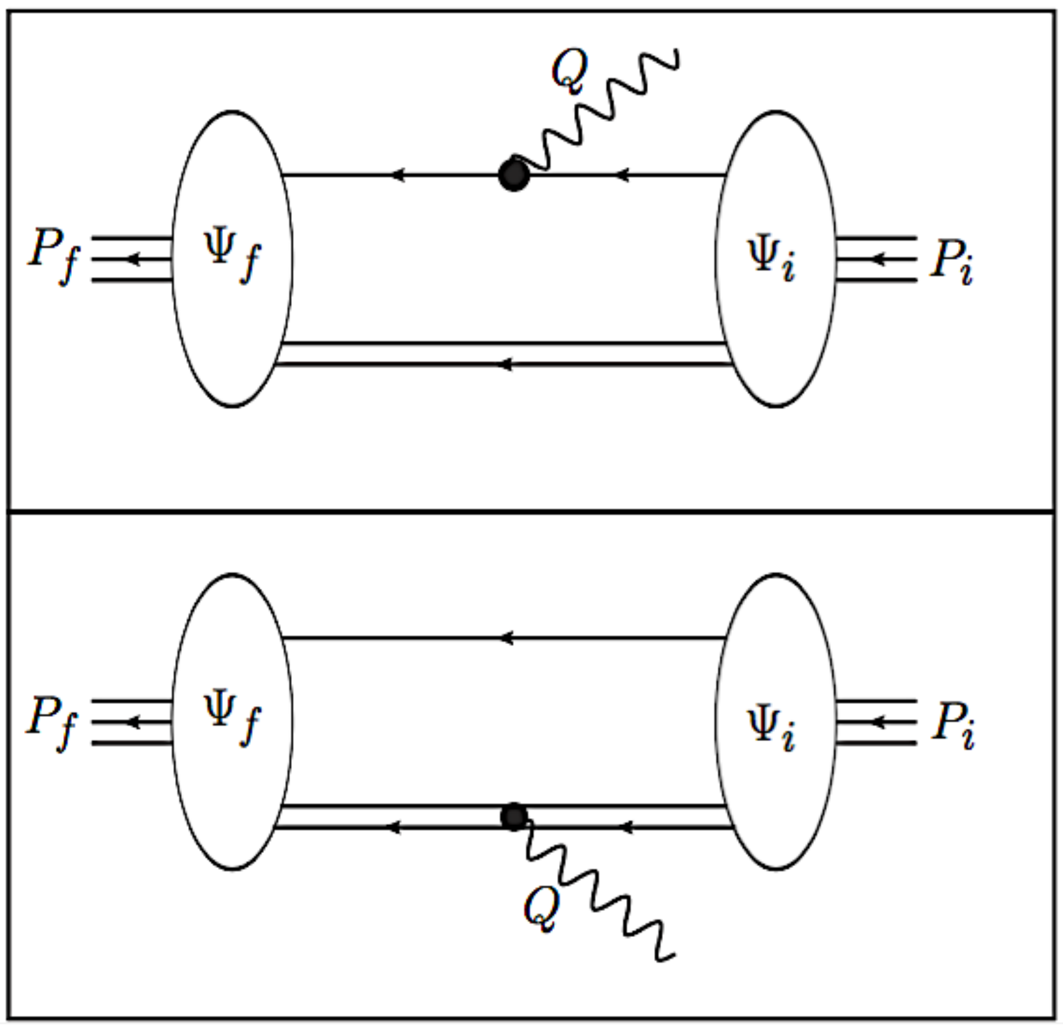

Contributions coming from **d-quark**

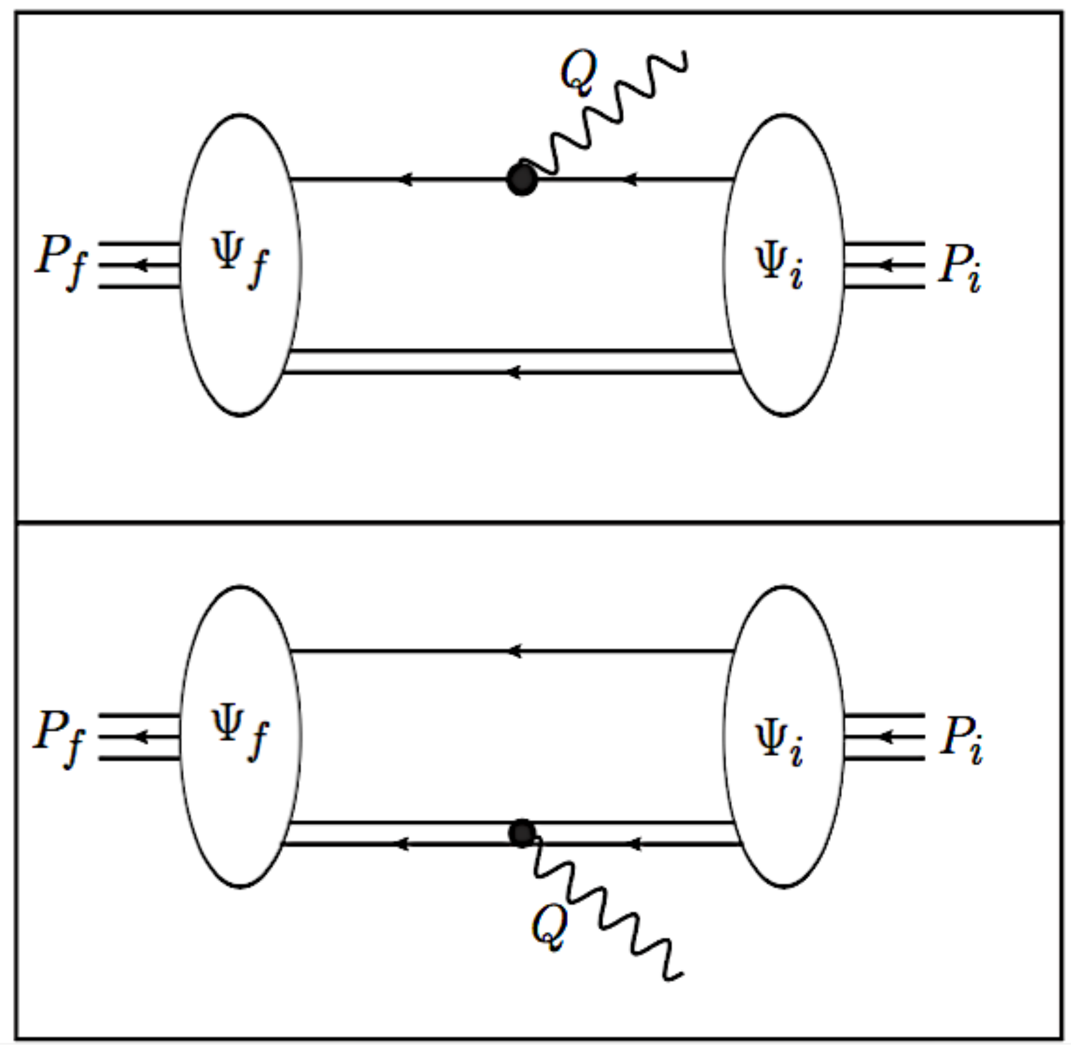

A world with scalar and axialvector diquarks

J. Segovia & C. D. Roberts
Phys. Rev. C94 (2016)

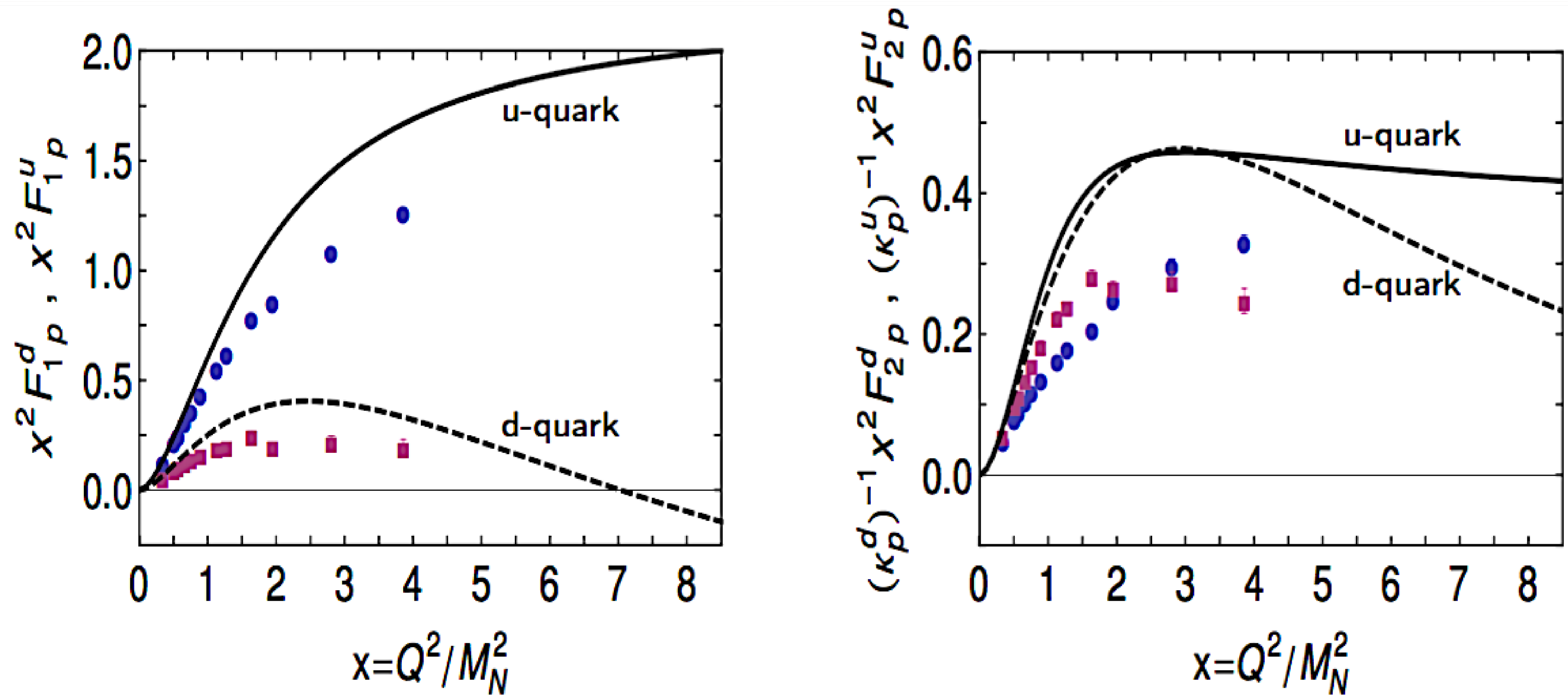

☞ Observations:

- F_{1p}^d is suppressed with respect F_{1p}^u in the whole range of momentum transfer.
- The location of the zero in F_{1p}^d depends on the relative probability of finding 1^+ and 0^+ diquarks in the proton.
- F_{2p}^d is suppressed with respect F_{2p}^u but only at large momentum transfer.
- There are contributions playing an important role in F_2, like the anomalous magnetic moment of dressed-quarks or meson-baryon final-state interactions.

Scalar and axialvector diquark contributions

J. Segovia & C. D. Roberts
Phys. Rev. C94 (2016)

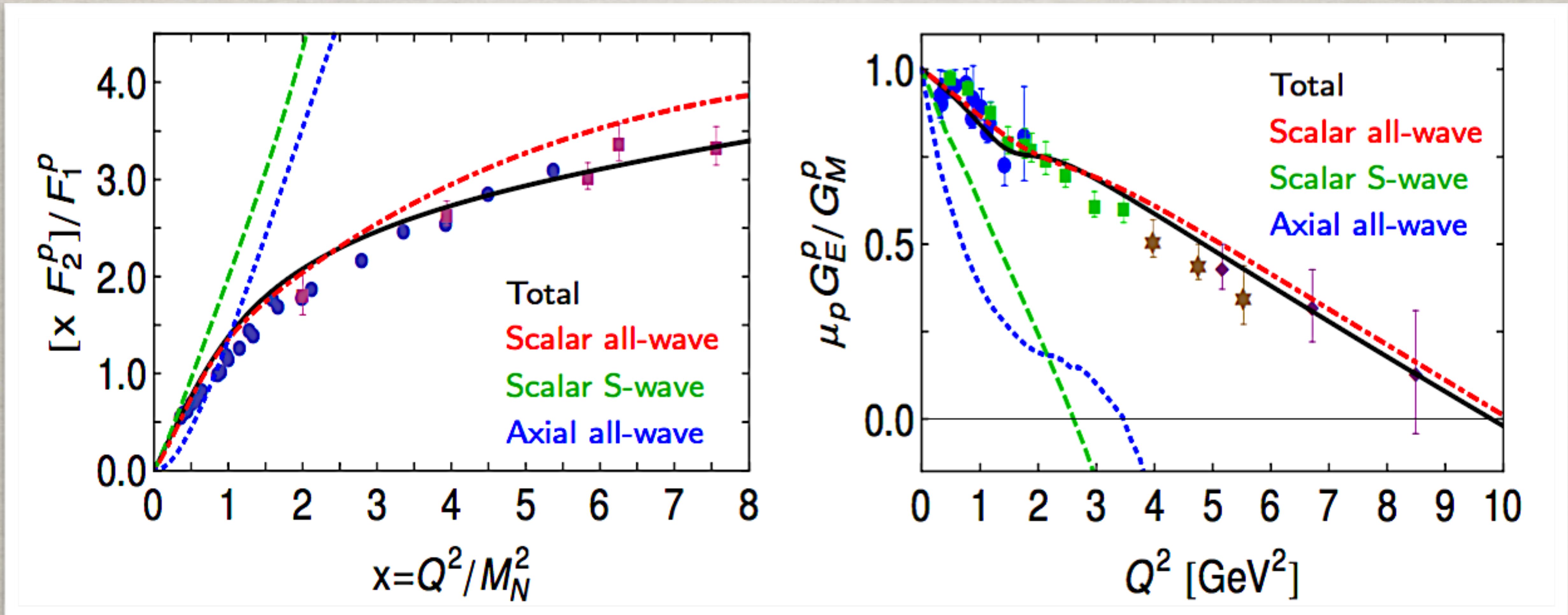

- Axialvector diquark contribution is not enough in order to explain the proton's electromagnetic ratios.
- *Scalar diquark contribution is dominant* and responsible of the Q^2-behavior of the the proton's e.m. ratios.
- Higher quark-diquark angular momentum components of the nucleon are critical in explaining the data.

The presence of higher orbital angular momentum components in the nucleon is an inescapable consequence of solving a realistic Poincaré-covariant Faddeev equation

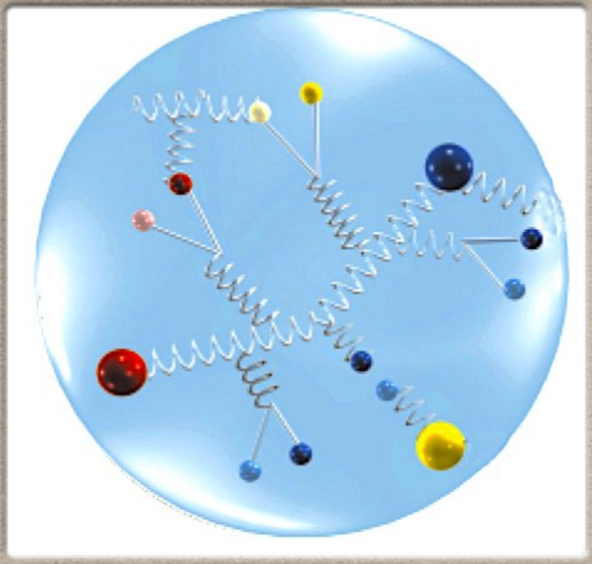

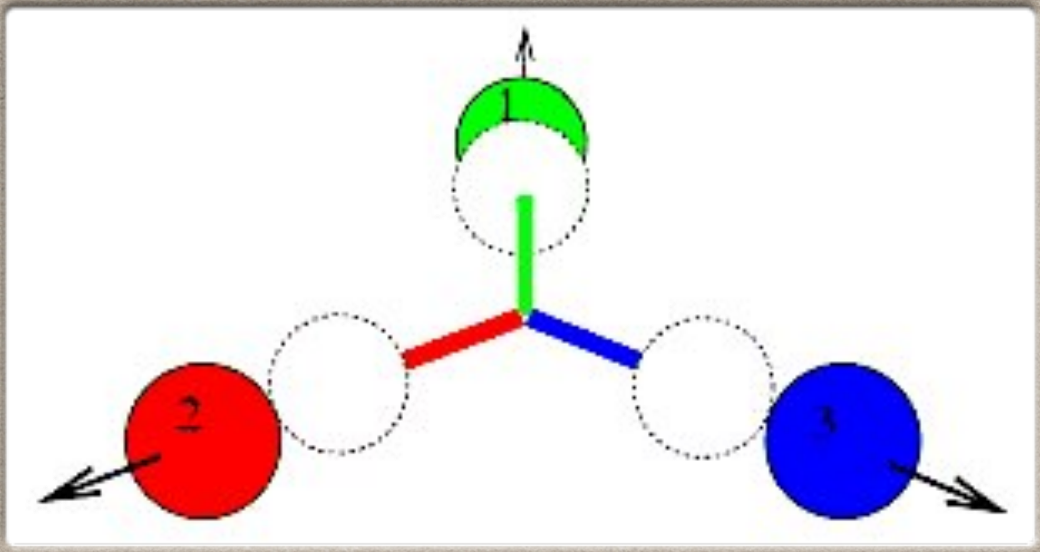

The Roper

PRL **104,** 042302 (2010) PHYSICAL REVIEW LETTERS week ending 29 JANUARY 2010

Disentangling the Dynamical Origin of P_{11} Nucleon Resonances

N. Suzuki,[1,2] B. Juliá-Díaz,[3,2] H. Kamano,[2] T.-S. H. Lee,[2,4] A. Matsuyama,[5,2] and T. Sato[1,2]

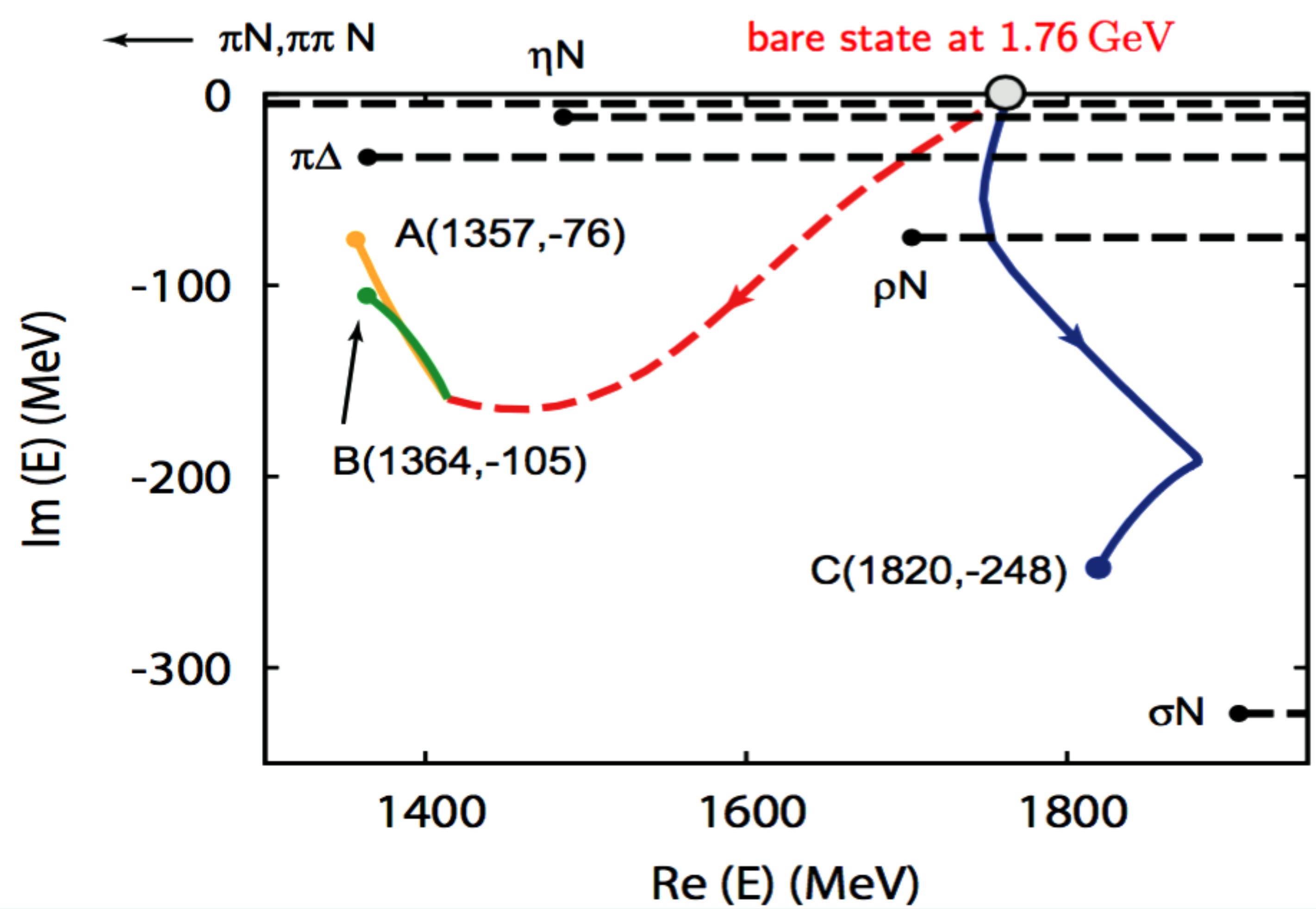

- EBAC examined dynamical origins of two poles associated with the *Roper resonance*.
- Both of them, together with the *next higher resonance in the P_{11} partial wave* have the same originating bare state.
- The meson cloud shields quark-core state and diminishes its mass considerably.

Ground and Radially Excited States of the Nucleon

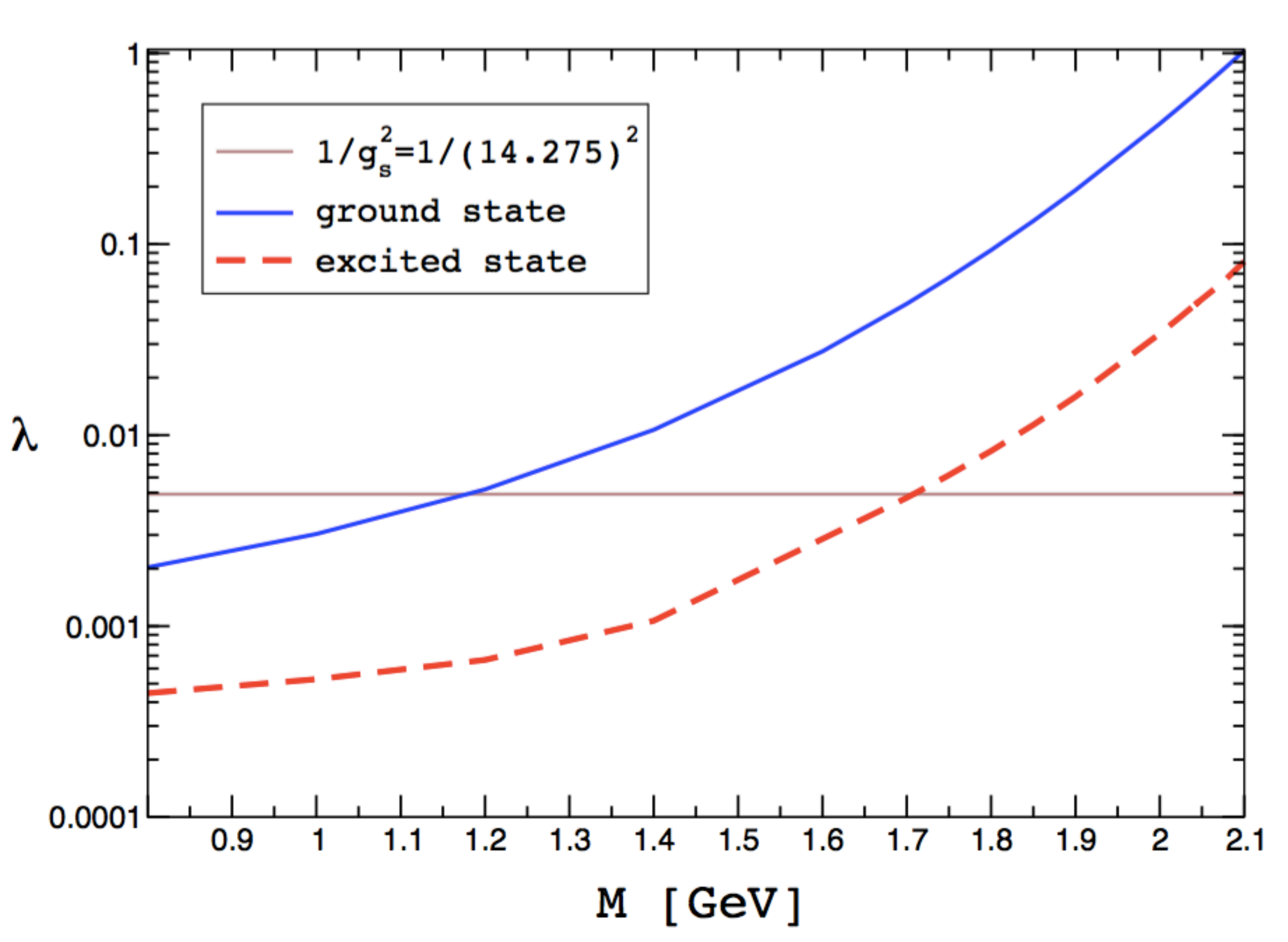

Roper Quark-Core Mass

	$R^{DSE}_{q(qq)}$	$R^{DSE}_{q(qq)}$	R^{DSE}_{qqq}	$R^{Contact}_{core}$	R^{DCCM}_{bare}
mass [GeV]	1.73	1.45	1.50	1.72	1.76

DSE: Faddeev quark-diquark amplitude of 1st excited state with dressed quark propagators.

J. Segovia, B. El-Bennich, E. Rojas, I.C. Cloët, C.D. Roberts, S.-S. Xu, H.-S. Zhong, Phys. Rev. Lett. 115 (2015)

G. Eichmann, C. Fischer, H. Sanchis-Alepuz, Phys.Rev. D94 (2016)

DSE: Faddeev three-quark interaction amplitude of 1st excited state with dressed propagators.

G. Eichmann, C. Fischer, H. Sanchis-Alepuz, Phys.Rev. D94 (2016)

Contact : Faddeev amplitude of 1st excited state with contact interaction gap equation.

D.J. Wilson, I. C. Cloët, L. Chang, C.D. Roberts, Phys. Rev. C85 (2012)

DCCM : Dynamical Coupled Channel Model.

N. Suzuki, B. Julio-Díaz, H. Kamano, T.-S. H. Lee, A. Matsuyama, T. Sato, Phys. Rev. Lett. 104 (2010)

Chebyshev Moments

First three Chebyshev moments of leading S_1 component of 1st excited state's Faddeev amplitude

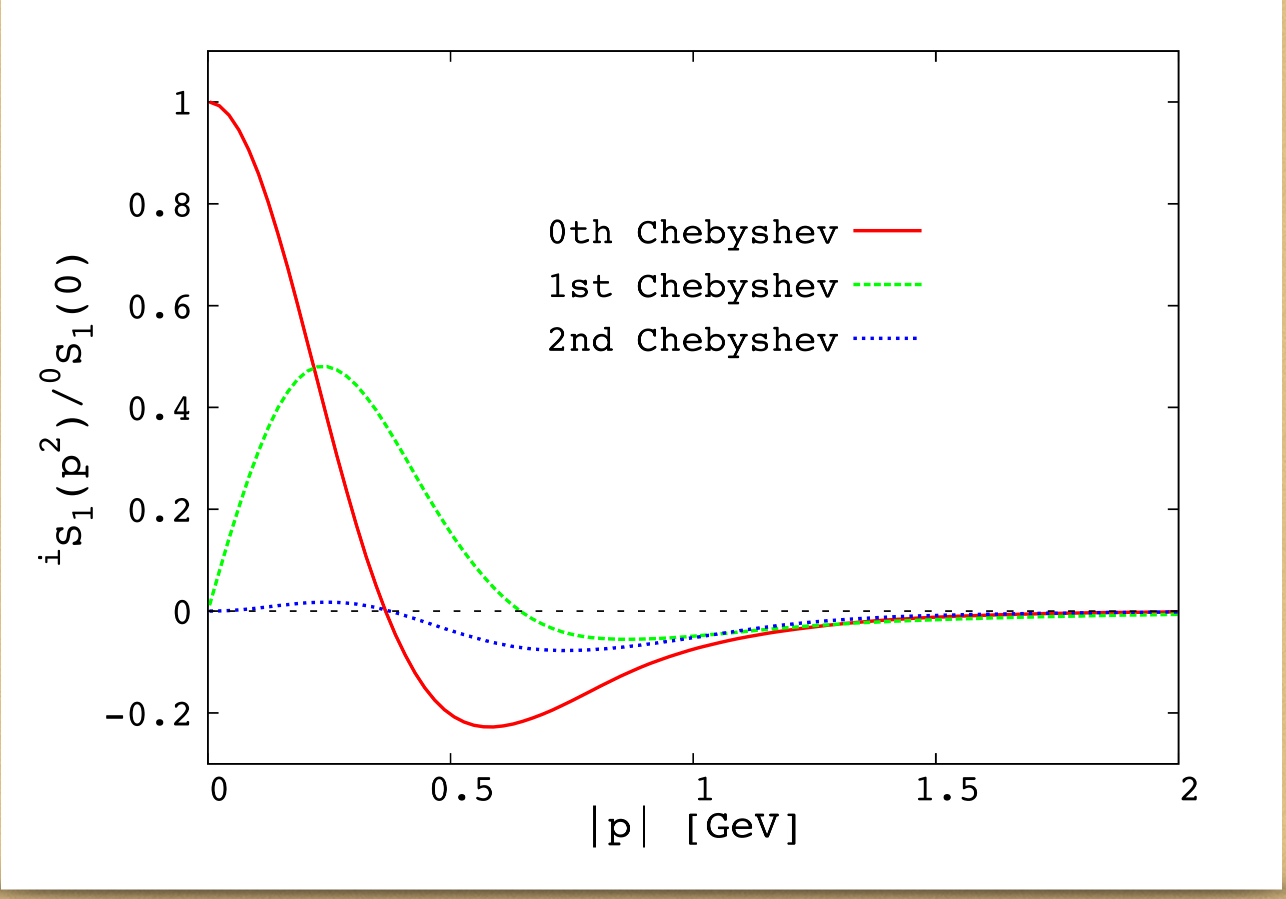

Chebyshev Moments

First three Chebyshev moments of leading S_1 component of 1st excited state's Faddeev amplitude

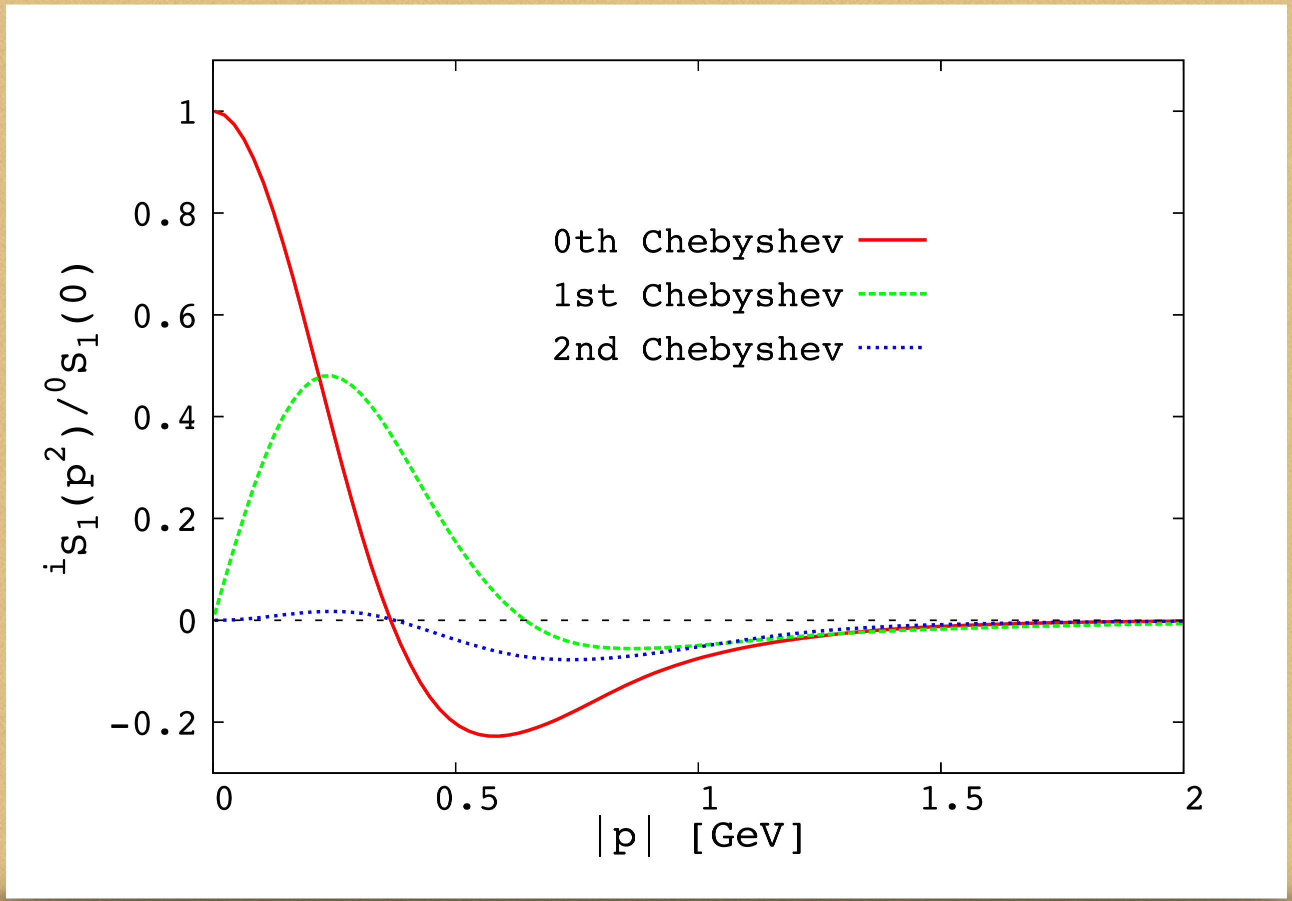

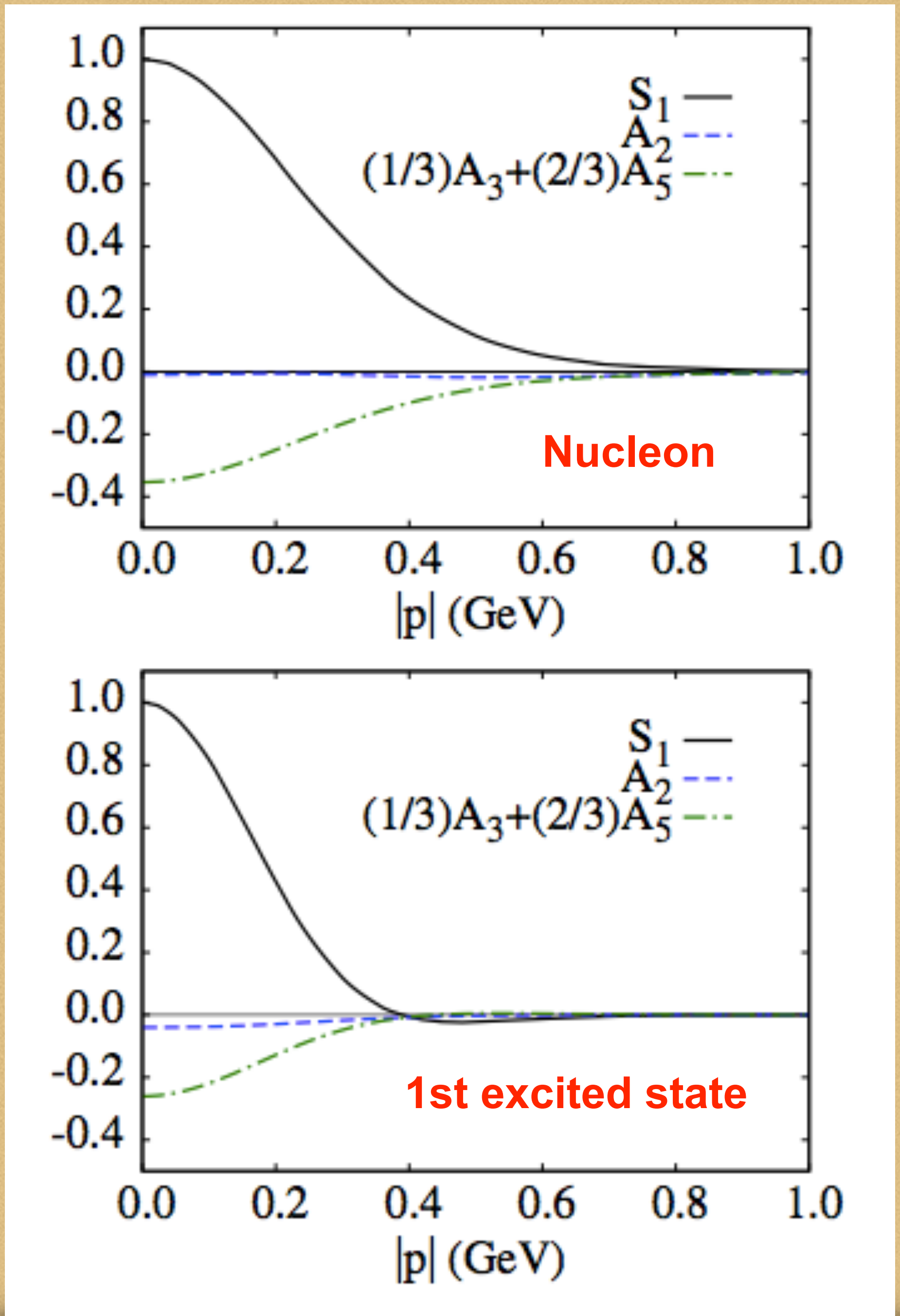

Zeroth Chebyshev moments of all *S*-wave components in the Faddeev wave function.
S_1 is associated with the baryon's scalar diquark; A_2, A_3, A_5 associated with axialvector correlation.

$\gamma\, p \to R^{+}$ Dirac and Pauli Transition Form Factors

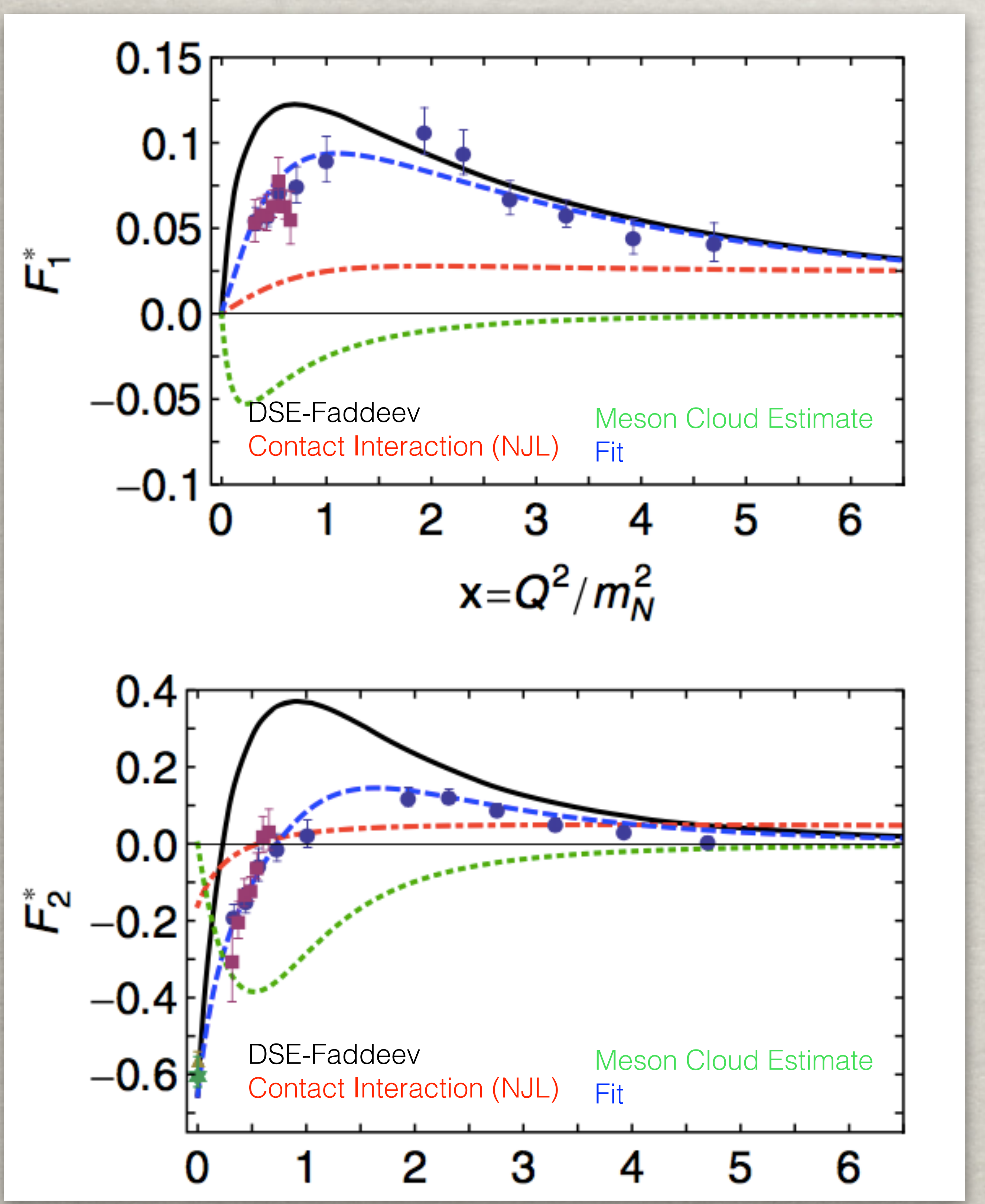

- Our calculation agrees quantitatively in magnitude and qualitatively in trend with the data on $x > 2$.
- The mismatch between our prediction and the data on $x = 2$ is due to meson cloud contribution.
- The dotted-green curve is an inferred form of meson cloud contribution from the fit to the data.
- The contact-interaction prediction disagrees both quantitatively and qualitatively with the data.

J. Segovia, B. El-Bennich, E. Rojas, I.C. Cloët, C.D. Roberts, S.-S. Xu, H.-S. Zhong, Phys. Rev. Lett. (2015)

$\gamma p \to R^{+}$ Dirac Transition Form Factor

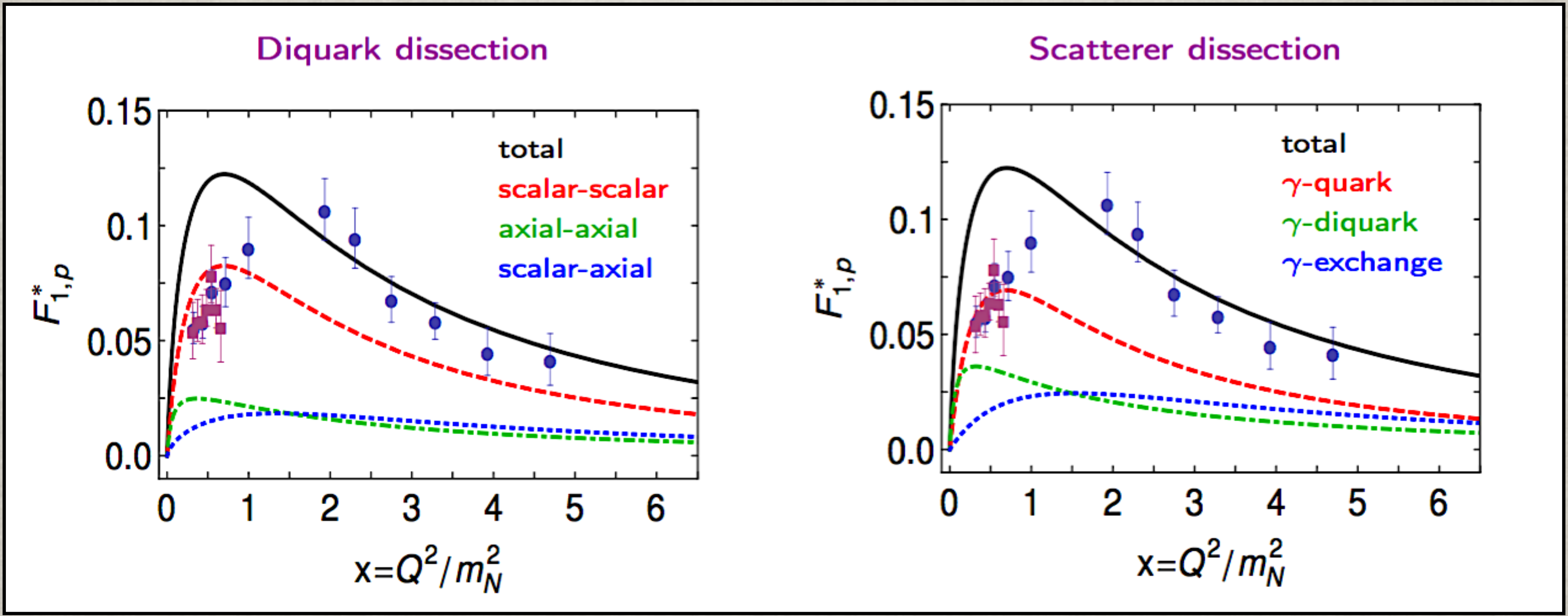

- The Dirac transition form factor is primarily driven by a photon striking a bystander dressed quark that is partnered by a scalar diquark.
- Lesser but non-negligible contributions from all other processes are found.
- In exhibiting these features, $F^*_{1p}(q^2)$ shows marked qualitative similarities to the proton's elastic Dirac form factor.

$\gamma p \to R^+$ Pauli Transition Form Factor

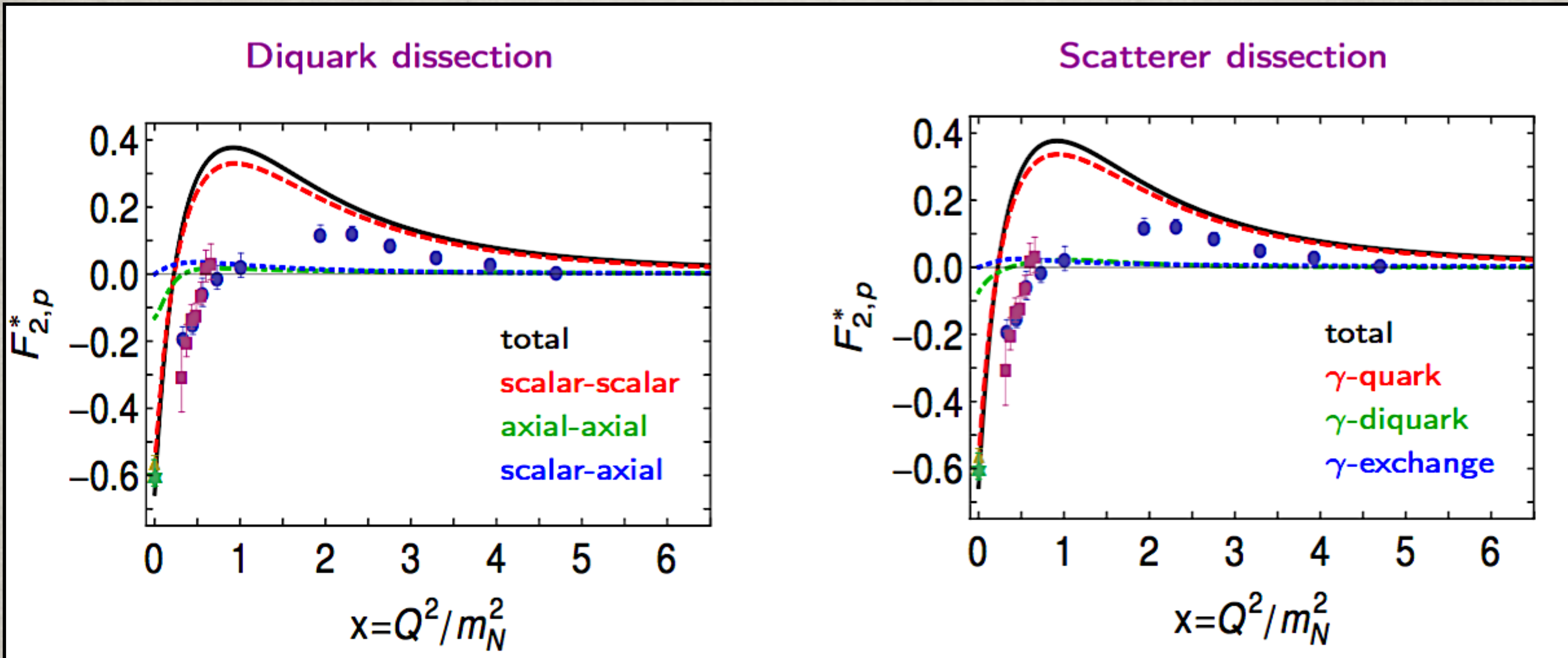

- A single contribution is overwhelmingly important: photon strikes a bystander dressed-quark in association with a scalar diquark.
- No other diagram makes a significant contribution.
- $F^*_{2p}(q^2)$ shows marked qualitative similarities to the proton's elastic Pauli form factor.

Nucleon & Parity Partner

Including pseudoscalar and vector *diquarks* …

- The *Nucleon* and *Roper* remain dominated by scalar and axialvector diquark correlation.
- Both, the *Nucleon* and *Roper* are dominated by *S*-waves (~75% & 85%).
- However, while the $N^*(1535)$ and $N^*(1650)$ are still dominated by scalar and axialvector correlations, the Faddeev amplitude is dominated by *P*-waves (~70% & 85%).

	$N_{n=0}$	$N_{n=1}$	$N^*_{n=0}$	$N^*_{n=1}$
$m^{\rm DSE}$	1.19	1.73	1.83	1.94
$m^{\rm expt.}$	0.94	1.44	1.54	1.65
$m^{\rm DSE} - m^{\rm expt.}$	0.25	0.29	0.29	0.29

$$m^*_N(1535) > m^*_N(1440)$$

C. Chen, B. El-Bennich, C. D.Roberts, S. M. Schmidt, J. Segovia and S. Wan
Phys. Rev. D **97**, no. 3, 034016 (2018)

$N^*(1535)$ & $N^*(1650)$

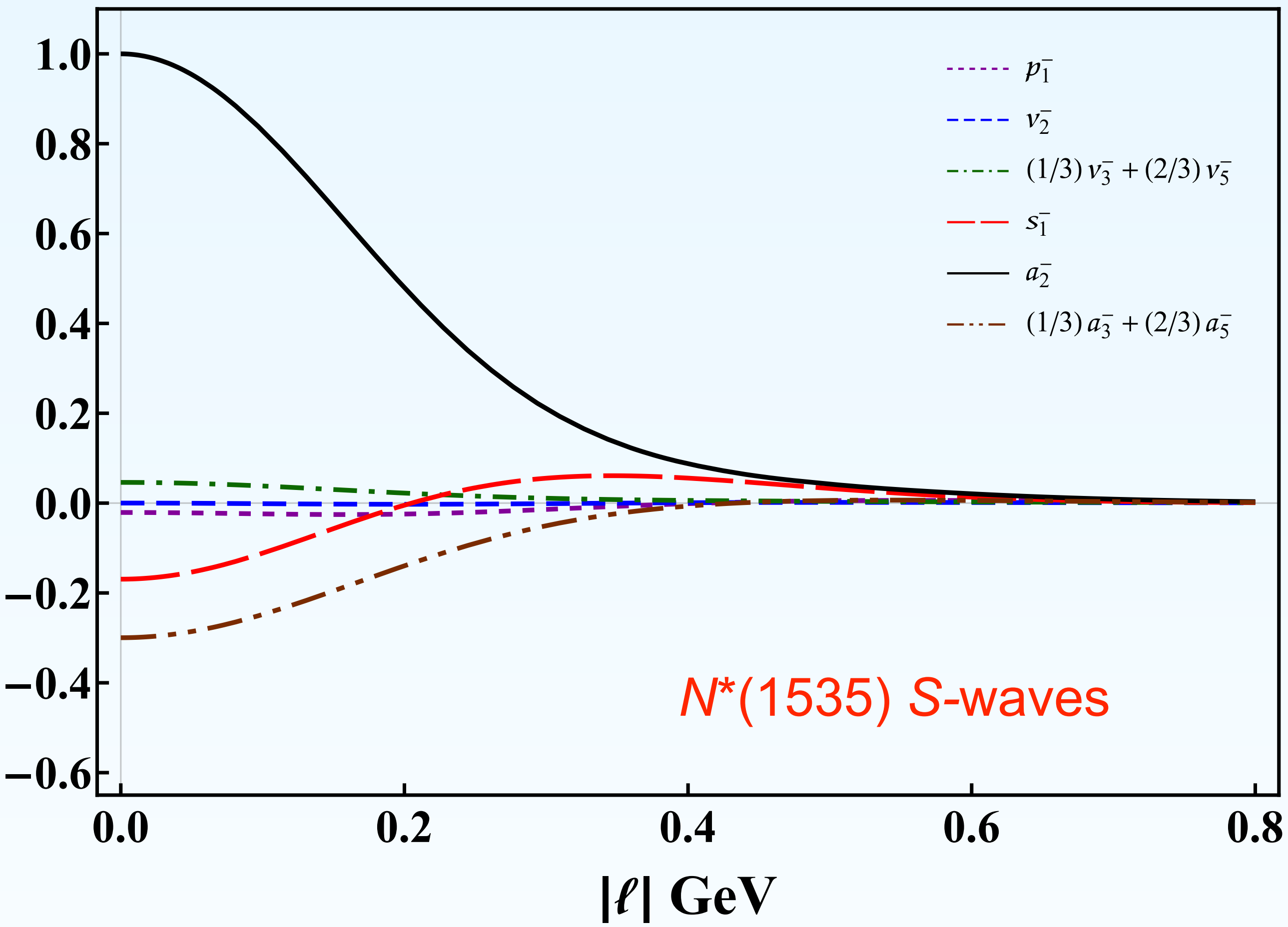

1.0
0.8
0.6
0.4
0.2
0.0
−0.2
−0.4
−0.6
0.0
0.2
0.4
0.6
0.8
|ℓ| GeV
p_1^-
v_2^-
$(1/3)\,v_3^- + (2/3)\,v_5^-$
s_1^-
a_2^-
$(1/3)\,a_3^- + (2/3)\,a_5^-$
N*(1535) S-waves

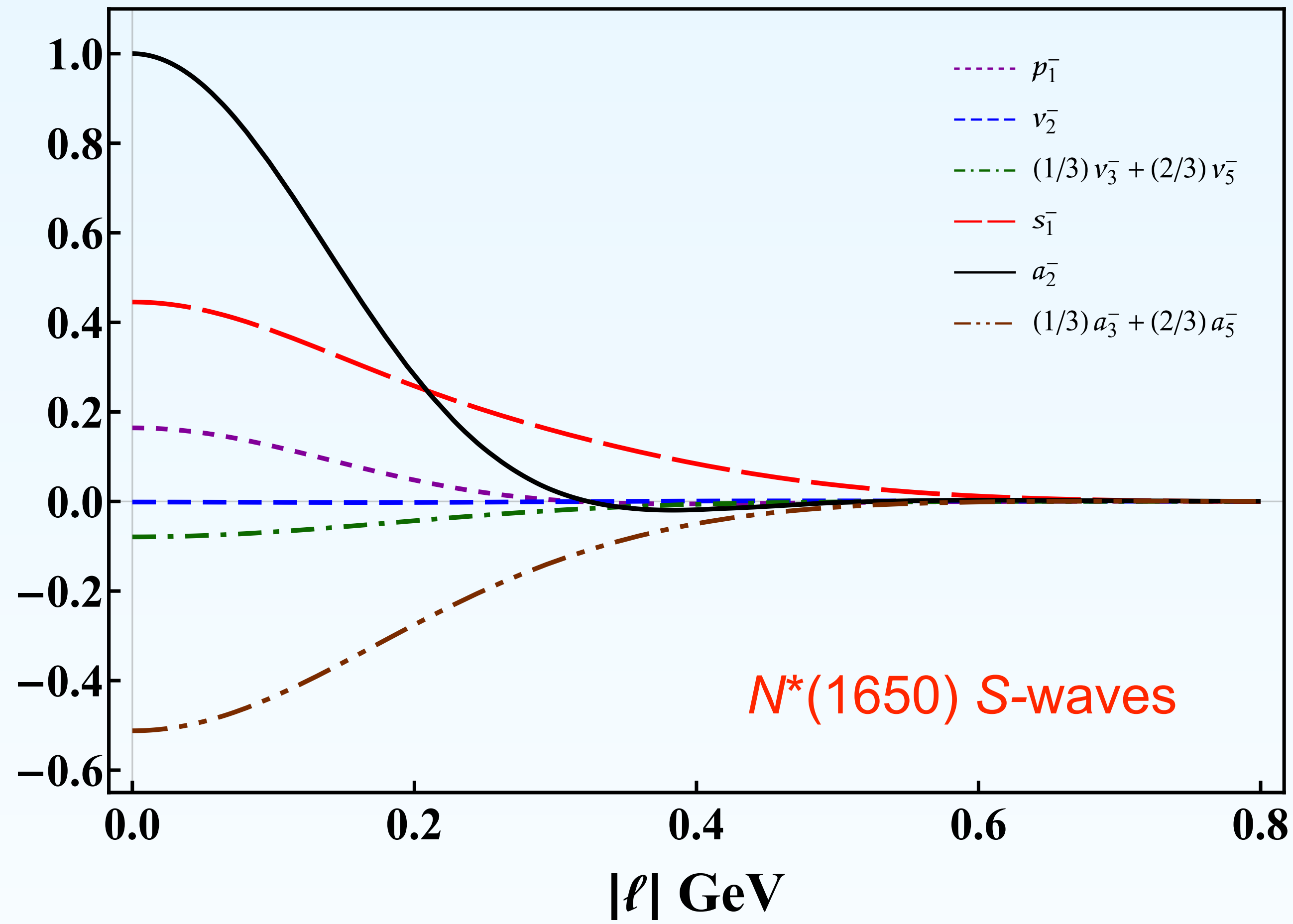

1.0
0.8
0.6
0.4
0.2
0.0
−0.2
−0.4
−0.6
0.0
0.2
0.4
0.6
0.8
|ℓ| GeV
p_1^-
v_2^-
$(1/3)\,v_3^- + (2/3)\,v_5^-$
s_1^-
a_2^-
$(1/3)\,a_3^- + (2/3)\,a_5^-$
N*(1650) S-waves

$N(940)$ & $N^*(1535)$ — P-waves

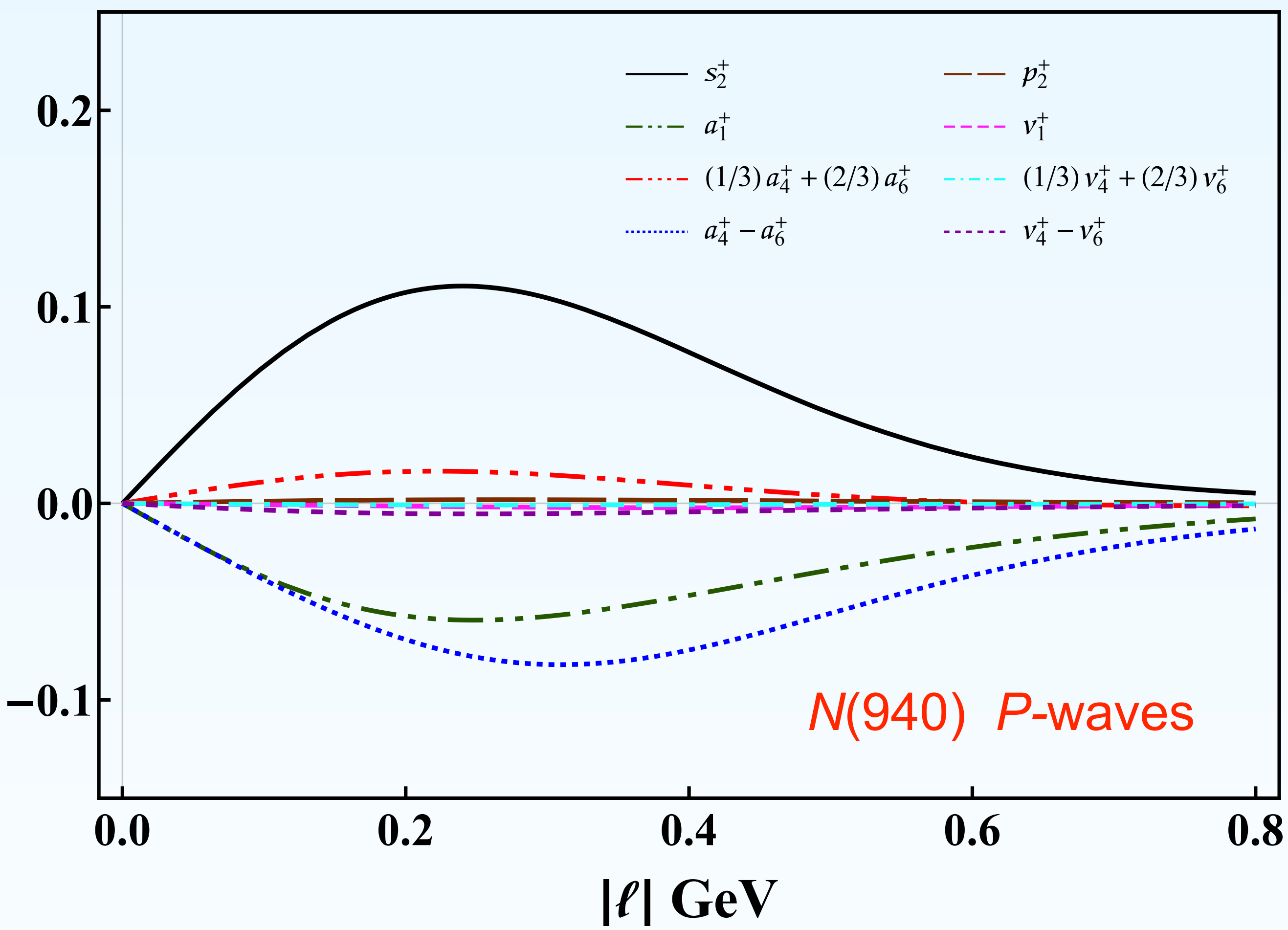

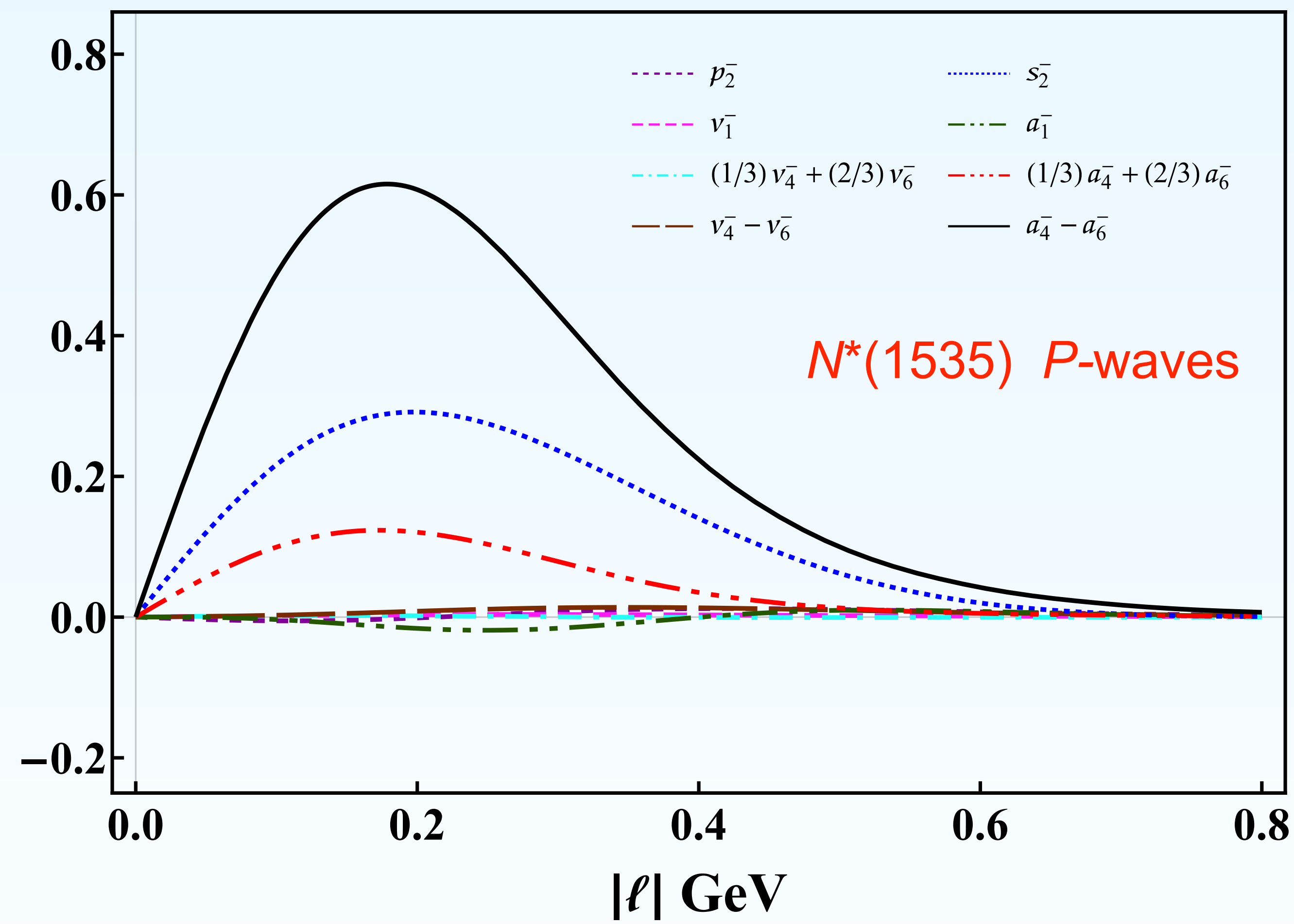

Baryon Octet & Decuplet

	N	Λ	Σ	Ξ	Δ	Σ^*	Ξ^*	Ω
m^{real}	1.14	1.28	1.35	1.46	1.39	1.51	1.64	1.76
m^{CI}	1.14	1.26	1.35	1.43	1.39	1.51	1.63	1.76
$m^{\text{expt.}}$	0.94	1.12	1.19	1.31	1.23	1.39	1.53	1.67
$m^{\text{real}} - m^{\text{expt.}}$	0.2	0.16	0.16	0.15	0.16	0.12	0.11	0.09
$m^{\text{real}} - m^{\text{CI}}$	0	0.02	0	0.03	0	0	0.01	0

CI : C. Chen, L. Chang, C. D. Roberts, S. Wan and D. J. Wilson, Few Body Syst. **53**, 293 (2012)

- Contact model is good enough to calculate the spectrum.
- However, in the CI model the Faddeev amplitudes are constant $\Rightarrow$ not suitable for quantitative predictions of large-q^2 form factors.

Baryon Octet & Decuplet

	N	Λ	Σ	Ξ	Δ	Σ^*	Ξ^*	Ω
m^{real}	1.14	1.28	1.35	1.46	1.39	1.51	1.64	1.76
m^{CI}	1.14	1.26	1.35	1.43	1.39	1.51	1.63	1.76
$m^{\text{expt.}}$	0.94	1.12	1.19	1.31	1.23	1.39	1.53	1.67
$m^{\text{real}} - m^{\text{expt.}}$	0.2	0.16	0.16	0.15	0.16	0.12	0.11	0.09
$m^{\text{real}} - m^{\text{CI}}$	0	0.02	0	0.03	0	0	0.01	0

CI : C. Chen, L. Chang, C. D. Roberts, S. Wan and D. J. Wilson, Few Body Syst. **53**, 293 (2012)

- Contact model is good enough to calculate the spectrum.
- However, in the CI model the Faddeev amplitudes are constant $\Rightarrow$ not suitable for quantitative predictions of large-q^2 form factors.

Conclusive Remarks

Conclusive Remarks

* We extracted the ground states and first radial excitations of the nucleon, its parity partner and hyperons using a quark-diquark Faddeev kernel that described the quark core.

* Dynamical chiral symmetry breaking and its correct implementation produces pions as well as strong electromagnetically-active diquark correlations.

* Poincaré covariance demands the presence of dressed-quark orbital angular momentum in the baryon.

* The presence of strong diquark correlations within the nucleon is sufficient to understand empirical extractions of the flavor-separated form factors.

* Scalar diquark dominance and the presence of higher orbital angular momentum components are responsible of the Q^2-behavior of $\mu_p G_E^p/G_M^p$ and F_2^p/F_1^p .

Conclusive Remarks about the Roper

- The Roper is the proton's first radial excitation. It's mass agrees with that of the bare unclothed Roper quark core.
- Our calculation agrees quantitatively in magnitude and qualitatively in trend with the data on $x \gtrsim 2$. The mismatch below $x \gtrsim 2$ is due to meson cloud contribution.
- Flavor-separated versions of transition form factors reveal that, as in the case of the elastic form factors, the d-quark contributions are suppressed with respect the u-quark ones.